eLife

Reviewed Preprint
v2 • March 13, 2025
Revised by authors

Reviewed Preprint
v1 • March 19, 2024

Structural Biology and Molecular Biophysics

Crosslinking by ZapD drives the assembly of short FtsZ filaments into toroidal structures in solution

Adrián Merino-Salomón, Jonathan Schneider, Leon Babl, Jan-Hagen Krohn, Marta Sobrinos-Sanguino, Tillman Schäfer, Juan R Luque-Ortega, Carlos Alfonso, Mercedes Jiménez, Marion Jasnin, Petra Schwille, Germán Rivas

Department of Cellular and Molecular Biophysics, Max Planck Institute of Biochemistry, Martinsried, Germany • Department of Molecular Structural Biology, Max Planck Institute of Biochemistry, Martinsried, Germany • Exzellenzcluster ORIGINS, Boltzmannstr. Garching, Germany • Molecular Interactions Facility, Centro de Investigaciones Biológicas Margarita Salas, Consejo Superior de Investigaciones Científicas (CSIC), Madrid, Spain • Cryo-EM facility, Max Planck Institute of Biochemistry, Martinsried, Germany • Centro de Investigaciones Biológicas Margarita Salas, Consejo Superior de Investigaciones Científicas (CSIC), Madrid, Spain • Helmholtz Pioneer Campus, Helmholtz Munich, Germany; Department of Chemistry, Technical University of Munich, Garching, Germany

eLife Assessment

The formation of the Z-ring at the time of bacterial cell division interests researchers working towards understanding cell division across all domains of life. The manuscript by Jasnin et al reports the cryoET structure of toroid assembly formation of FtsZ filaments driven by ZapD as the cross linker. The findings are **important** and have the potential to open a new dimension in the field, but the evidence to support these exciting claims is currently **incomplete**, mostly because of the suboptimal "resolution of the toroids", so in the absence of additional experiments, the interpretations would need to be toned down.

https://doi.org/10.7554/eLife.95557.2.sa3

Abstract

Bacterial cell division relies on the Z ring, a cytoskeletal structure that acts as a scaffold for the assembly of the divisome. To date, the detailed mechanisms underlying the assembly and stabilization of the Z ring remain elusive. This study highlights the role of the FtsZ-associated protein (Zap) ZapD in the assembly and stabilization of Z-ring-like structures via filament crosslinking. Using cryo-electron tomography and biochemical analysis, we show that, at equimolar concentrations of ZapD and FtsZ, ZapD induces the formation of toroidal structures composed of short, curved FtsZ filaments that are crosslinked vertically, but also laterally and diagonally. At higher concentrations of ZapD, regularly spaced ZapD dimers crosslink FtsZ filaments from above, resulting in the formation of straight bundles. Despite the simplicity of this reconstituted system, these findings provide valuable insights into the structural organization and stabilization of the Z ring by Zap proteins in bacterial cells,

revealing the key role of optimal crosslinking density and geometry in enabling filament curvature and ring formation.

Introduction

Cell division in bacteria is a well-orchestrated process mediated by a multiprotein complex called the divisome. Their components interact reversibly to form a division ring, which is essential for cytokinesis[1–3]. At the core of this process in most bacteria is FtsZ, a tubulin homolog that polymerizes in the presence of GTP beneath the inner membrane at the future division site, providing a scaffold for recruiting other division proteins[4–8]. FtsZ undergoes treadmilling due to polymerization-dependent GTP hydrolysis, allowing the ring to exhibit its dynamic behavior[9]. Depending on environmental conditions, FtsZ filaments can assemble into various structures, including bundles, sheets, and toroids[10–14]. Membrane-tethered FtsZ assemblies are arranged as loosely structured spirals in the midcell region, guided by spatial regulators. These structures eventually coalesce to form a cohesive Z ring[15].

The molecular components involved in cell division must be in the right place at the right time during the cell cycle. Several factors in this spatiotemporal regulation modulate FtsZ assembly. In *Escherichia coli*, FtsA and ZipA tether FtsZ to the membrane[16–18] and, together with a set of FtsZ-associated proteins (Zaps), stabilize the ring[19–22]. Conversely, negative modulators inhibit FtsZ assembly at other sites, namely Min proteins at the polar regions[23] and SlmA on the nucleoid[24]. Most of these modulators interact with FtsZ through its carboxy-terminal end, which modulates division assembly as a central hub[25,26]. ZapD is the only Zap protein known to crosslink FtsZ by binding its C-terminal domain, suggesting a critical Z ring structure stabilizing function[19,27–30] (**Fig. 1a**).

To date, a high-resolution structure of the Z ring remains unresolved. Most evidence suggests that FtsZ filaments are arranged in short patches along the equatorial circle, held together by lateral interactions and interactions with Zap proteins[2,7,31–33]. The dynamics of treadmilling and lateral interactions between FtsZ filaments, as well as crosslinking by FtsZ-associated proteins (Zaps), are thought to play a crucial role in the condensation of the Z ring[34]. Specifically, the crosslinking of filaments by Zaps, particularly ZapD, is vital for maintaining the neighboring organization of the filaments into a ring structure. This organization may also be critical for the functionality of the divisome and the mechanism of force generation during cytokinesis[1,2,7,35–38].

Zap proteins play overlapping roles in stabilizing the Z ring during cell division. Although they are non-essential for division, their absence leads to less compact Z rings, and the know-out of two or more Zap encoding genes simultaneously results in cell elongation[19,39,40]. Notably, these different Zap proteins do not share any sequence homology and differ in their structure and filament crosslinking mechanism[20,27,41]. Additionally, Zap proteins may actively remove FtsZ from the septum during the final stages of constriction[42]. They also facilitate the positioning of the Z ring at the replication terminus of the chromosome by interacting with MatP, which forms a scaffolding anchor known as Ter-linkage[43].

ZapD is a symmetrical dimer consisting of an α-helical domain and a β-sheet domain containing a positively charged binding pocket required for crosslinking and bundling FtsZ filaments[30,41]. ZapD binds to the C-terminal region of FtsZ through electrostatic interactions[30]. ZapD crosslinks FtsZ filaments, promoting bundling and significantly reducing the GTPase activity of FtsZ[19]. A model of how ZapD crosslinks neighboring FtsZ filaments has been proposed based on the structural analysis of ZapD-FtsZ interactions[41]. In this model, the ZapD dimer connects two FtsZ

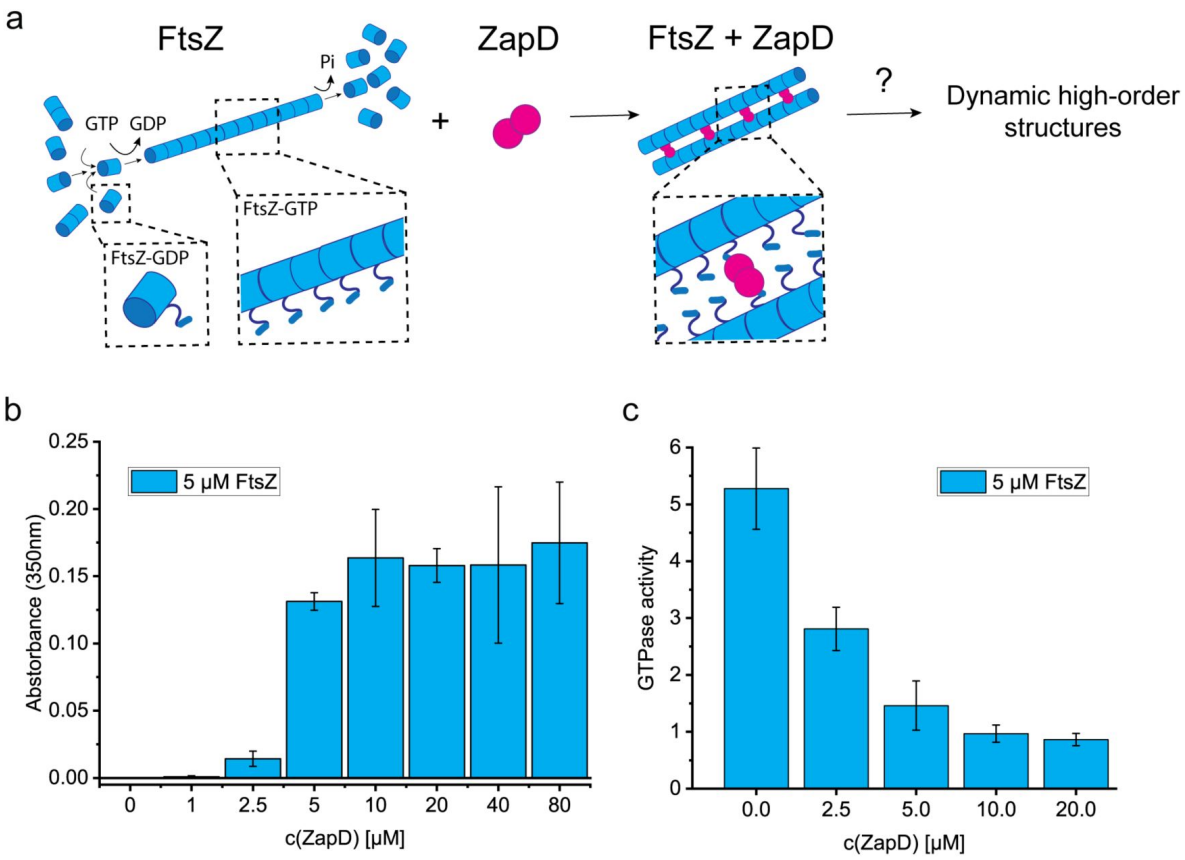

Figure 1.

ZapD binds FtsZ and promotes filament bundling.

a. Scheme of the FtsZ protein and its interaction with ZapD. E. coli FtsZ (blue) monomers in solution oligomerize depending on the buffer conditions. Upon GTP binding, FtsZ homopolymerizes directionally, assembling single stranded filaments. ZapD is a robust dimer (magenta) that interacts directly with FtsZ, crosslinking filaments by promoting lateral interactions between them. Although the molecular mechanism is still unclear, the current hypothesis of interaction assumes dimers of ZapD crosslinking two FtsZ filaments through the C-terminal region of FtsZ, expecting at around 1:1 (FtsZ:ZapD) molar ratio in an homogeneous bundle (1 dimer of ZapD connected to 2 monomers of FtsZ). According to this model, the orientation of the FtsZ filaments could be parallel or antiparallel, allowing the growth and treadmilling of the filaments. However, the mechanism of assembly of dynamic high-order structures is still unknown.
b. Turbidity assays measuring the absorbance at 350 nm of samples containing 5 μM FtsZ and increasing concentrations of ZapD. The turbidity of the sample was measured 5 minutes after the addition of 1 mM GTP at working buffer (50 mM KCl, 50 mM Tris-Cl, 5 mM $MgCl_2$ pH 7). FtsZ polymers do not show a significant turbidity at this wavelength; therefore, the signal at 350 nm corresponds to the presence of large FtsZ macrostructures and bundles. The mean value and SD of >3 independent replicates are plotted in the graph.
c. GTPase activity of FtsZ after addition of 1 mM GTP in presence of increasing concentrations of ZapD at working conditions (50 mM KCl, 50 mM Tris-Cl, 5 mM $MgCl_2$ pH 7). The mean value and SD plotted in the graph are the result of 3 independent replicates. The GTPase activity was measured as a result of the Pi released from GTP consumption. The units are Mol GTP consumed per Mol FtsZ per min.

filaments through the C-terminal domain, which could organize them in a parallel or antiparallel orientation due to the flexibility provided by the flexible linker (**Fig. 1a**). However, the experimental validation of this model is still missing.

Furthermore, the link between FtsZ bundling, promoted by ZapD, and the large-scale organization of FtsZ filaments remains unresolved. Therefore, investigating how ZapD crosslinks FtsZ filaments may shed light on the molecular mechanisms underlying Z ring assembly. Recently, Gong et al.[44] demonstrated that although the FtsZ crosslinking proteins are not individually essential, they collectively play a critical role in the condensation and stability of the Z ring in different organisms. However, the specific mechanisms driving this condensation remain unclear, highlighting the complexity of the bacterial cell division process.

In this study, we used cryo-electron microscopy (cryo-EM) and cryo-electron tomography (cryo-ET), together with biochemical and biophysical assays, to investigate the structural organization of FtsZ polymers in the presence of ZapD. This integrated approach revealed that, at equimolar concentrations of ZapD and FtsZ, ZapD facilitates the assembly of FtsZ filaments into toroidal polymers in solution. This observation is consistent with the low resolution structure of the Z-ring obtained *in vivo*[7,45–47]. Our results allowed us to propose a molecular mechanism for toroid formation, providing valuable insights into how crosslinking of division proteins drives the stabilization of the Z-ring.

Results

ZapD dimer interacts with FtsZ-GDP oligomers

Previous structural studies have identified a direct interaction between ZapD and FtsZ through the C-terminal domain or central hub of FtsZ, involving charged residues in the interaction[28,30]. To independently verify these findings, we investigated the interaction between FtsZ-GDP and ZapD using analytical ultracentrifugation (AUC) (see Supplementary Fig. 1). First, we confirmed that ZapD forms stable dimers, which is consistent with previous studies[19,28,41] (Supplementary Fig. 1a (I) and b). In contrast, unpolymerized FtsZ-GDP primarily self-assembles from monomers into dimers and other oligomeric species, albeit in small proportions, as expected[48]. (Supplementary Fig. 1a (II)).

Sedimentation velocity analysis of mixtures of the two proteins revealed the presence of two predominant molecular species of ZapD:FtsZ complexes in solution. These complexes are compatible with ZapD dimers bound to one or two FtsZ monomers, corresponding to ZapD:FtsZ stoichiometries of 2:1 and 1:1, respectively (Supplementary Fig. 1a (III-IV)). This observation is consistent with the proposed interaction model[41]. Furthermore, we confirmed the interaction of both proteins using fluorescence anisotropy and fluorescence correlation spectroscopy (Supplementary Fig. 2a and b). In these experiments, an increase in fluorescence anisotropy or diffusion time suggested the formation of larger particles due to protein-protein interactions.

ZapD binding promotes the bundling of FtsZ-GTP polymers

ZapD is a crosslinker for FtsZ filaments, promoting their bundling in solution[19]. However, the precise molecular mechanism by which ZapD crosslinks the filaments remains unclear. To investigate the biochemical features underlying this bundling process, we examined how the formation of large FtsZ bundles or higher-order FtsZ polymer structures depends on the concentration of ZapD. For this analysis, we used turbidity measurements at 350 nm. When testing GTP-FtsZ filaments at 5 or 10 μM concentrations, we found negligible turbidity, similar to that of ZapD alone at concentrations ranging from 1 to 40 μM. However, when ZapD was added, the

turbidity of the FtsZ polymers increased, reaching a maximum at approximately 5 μM of ZapD (with a ZapD-FtsZ molar ratio of around 1). This turbidity level did not change significantly even at higher ZapD concentrations. (**Fig. 1b** and Supplementary Fig. 3).

In the presence of ZapD, FtsZ rapidly forms higher order polymers upon addition of GTP, as indicated by turbidity assays. In contrast, the formation of single-or double-stranded FtsZ filaments without ZapD does not result in a significant increase in turbidity. Compared to FtsZ filaments observed in vitro, FtsZ bundles with ZapD exhibited reduced GTPase activity, reaching 20% at equimolar or higher concentrations of ZapD (**Fig. 1c**, Supplementary Fig. 4), in agreement with previous studies[19]. The macrostructures formed by FtsZ in the presence of ZapD were disassembled more slowly than the FtsZ filaments upon GTP consumption (Supplementary Fig. 3). Replenishment of GTP allowed for a partial recovery of the turbidity signal, suggesting that the FtsZ bundles can be rapidly reassembled (Supplementary Fig. 3e). Previous studies have shown that high concentrations of macromolecular crowders (such as Ficoll or dextran) promote the formation of dynamic FtsZ polymer networks[13], observations that are consistent with our results. In these cases, the GTPase activity of FtsZ was significantly reduced compared to that of FtsZ filaments, leading to a decrease in GTPase turnover. Similar mechanisms may apply to assembly reactions involving ZapD[19,28].

To understand the relationship between the concentration dependence of the turbidity signal – associated with the formation of FtsZ bundles or higher order structures driven by ZapD (see **Fig. 1b**) – and the amount of ZapD bound to the FtsZ binding sites, we carried out analytical centrifugation sedimentation velocity assays, previously used to characterize the binding of ZapD to GDP-FtsZ. This method allowed us to separate ZapD-FtsZ bundles from free ZapD in solution and calculate the concentration of unbound ZapD from the interference signal of the slowly sedimenting protein behind the rapidly sedimenting heavy ZapD-FtsZ complexes. Using the measured concentration of free ZapD together with known input concentrations of ZapD and FtsZ, we were able to calculate the concentration of bound ZapD and the binding density of ZapD in the bundles (moles of bound ZapD dimer per mole of FtsZ monomer) at different total concentrations of ZapD. Our results showed that in the 5-10 μM ZapD concentration range, the bundles exhibited an estimated ZapD binding density of approximately 0.2, meaning that one ZapD dimer is associated with every four to six FtsZ monomers. In contrast, at higher ZapD concentrations (30-40μM), the binding density increased to 0.5, indicating one ZapD dimer for every two FtsZ monomers. These results are consistent with parallel co-sedimentation assays and additional analysis by SDS-PAGE, demonstrating an enrichment of ZapD in the pellet containing the FtsZ bundles at elevated ZapD concentrations (see Supplementary Fig. 5).

These results suggest that the ZapD binding density in the polymers increases with higher ZapD concentrations. We then carried out cryo-electron microscopy (cryo-EM) and cryo-electron tomography (cryo-ET) studies to investigate whether this increase in binding density affects the structural organization of the bundles formed.

ZapD facilitates the formation of higher order FtsZ-GTP toroidal structures

Previous studies have visualized bundles with similar features using negative-stain transmission electron microscopy[19,30,41]. Here, cryo-EM allowed us to avoid any staining artifact or structural distortion (due to adsorption or flattening upon grid drying[49]) and to resolve single filaments. In the presence of GTP, FtsZ polymerized into thin filaments of variable length and curvature (**Fig. 2a**). Upon addition of equimolar amounts of ZapD, corresponding to the slightly substoichiometric ZapD binding densities described in the previous section, FtsZ filaments assembled into bundles that predominantly formed circular toroidal structures (**Fig. 2b, c** and Supplementary Fig. 6a), making them a compelling study target. A close-up view of the FtsZ toroid suggests a partially ordered arrangement of the filaments in the toroidal structure (**Fig. 2c**).

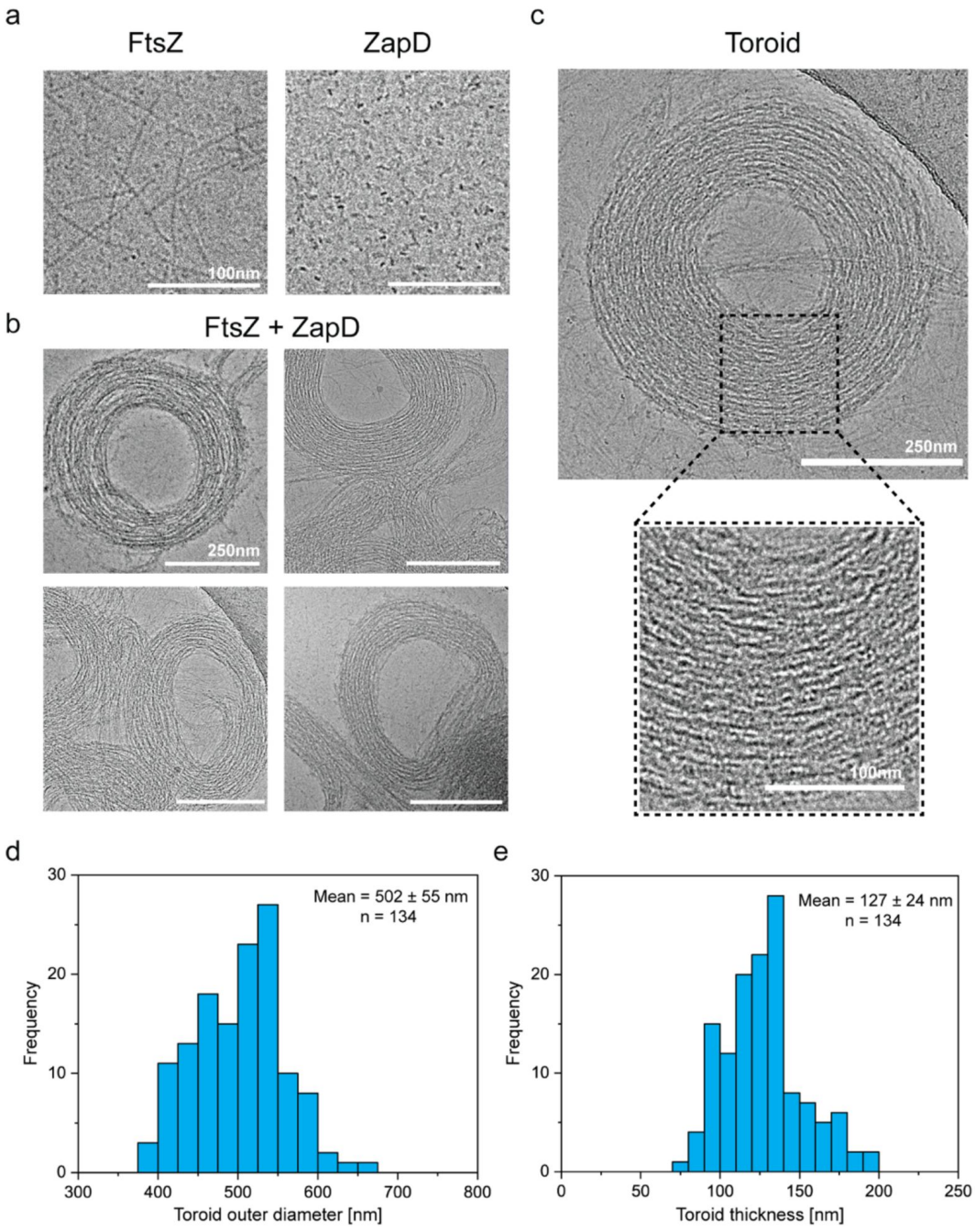

Figure 2.

ZapD promotes the formation of FtsZ toroids.

a. ~~ Cryo-EM micrographs of FtsZ filaments (FtsZ-GTP form) (left) and ZapD protein (right) at 10 μM under working conditions (50 mM KCl, 50 mM Tris-Cl, 5 mM $MgCl_2$ pH 7). Scale bars are 100 nm
b. Cryo-EM images of FtsZ (10 μM) in the presence of equimolar concentrations of ZapD (ratio 1:1) and 1 mM GTP in working conditions. Cryo-EM grids were plunge frozen 2 min after GTP addition to favor the assembly of FtsZ and ZapD structures. The proteins were mixed before the polymerization was triggered by GTP addition. Scale bars are 250 nm.
c. Micrograph of an individual FtsZ toroid found under the same conditions as in (**b**). Close-up view of an area within the toroid is framed by a dotted black line, revealing the large amount of FtsZ filaments that form its structure.
d. Distribution of the outer diameter of the FtsZ toroid. Each toroid was measured perpendicularly in the shortest and longest axis to ensure the reliability of the measurement. The mean value and standard deviation are shown in the graph.
e. Distribution of toroidal thickness. It was measured as the result of the difference between the outer and inner diameter of each toroid. The mean value and standard deviation are shown in the graph.

Quantitative analysis of the toroidal structure revealed a conserved organization, with an outer diameter on the order of the bacterial cell size (502 ± 55 nm) (**Fig. 2d**), a typical thickness of 127 ± 25 nm (**Fig. 2e**) and an average height of 93 ± 15 nm (Supplementary Fig. 6b). By measuring the shortest and longest axes, we determined that the circularity of the structure was 0.92 ± 0.1 and 0.85 ± 0.1 for the outer and inner diameters, respectively (Supplementary Fig. 6c). This conserved toroidal structure could result from the intrinsic curvature of the FtsZ filaments[10,31,50] stabilized by ZapD binding. The dimension of a ZapD dimer is ~7 nm along its longest axis. Huecas et al.[31] estimated an interfilament distance of ~6.5-6.7 nm for toroids of *Bacillus subtilis* FtsZ. These authors also observed a difference in this distance as a function of the linker, suggesting that linker length modulates FtsZ-FtsZ interactions. We observed a similar spacing for double filaments (5.9 ± 0.8 nm) and a longer spacing in the presence of ZapD (7.88 ± 2.1 nm). Previous studies with ZapD have suggested that distances of 6-12 nm are possible based on the protein structure[41]. Longer linkers may also provide additional freedom to spread the filaments further apart and allow a greater degree of variability in the connections made by ZapD.

Previous studies have shown different FtsZ structures at different concentrations and buffer conditions. FtsZ filaments are flexible and can generate different curvatures ranging from mini rings of ~24 nm to intermediate circular filaments of ~300 nm or toroids of ~500 nm in diameter (reviewed in[50,51]). It is reasonable to assume that FtsZ filaments can accommodate the toroidal shape promoted by ZapD crosslinking.

Our data showed that ZapD dimers crosslink adjacent FtsZ filaments into bundles and toroids. These toroids are remarkably regular in size and similar to the bacterial diameter[7,45,46], suggesting a conserved intrinsic curvature of the FtsZ filaments across a range of ZapD bonds[50].

3D structure of ZapD-mediated FtsZ toroids revealed by cryo-ET

Visualization of toroidal FtsZ structures using cryo-EM revealed a complex arrangement of FtsZ filaments within the toroidal shape (**Fig. 2c**). To gain a more detailed understanding of their three-dimensional (3D) organization, we used cryo-ET. Our initial analysis focused on ZapD-mediated toroidal FtsZ structures at equimolar concentrations of ZapD and FtsZ (**Fig. 3** and Supplementary Fig. 7a).

Cryo-ET revealed the dense packing of the toroidal structures, with numerous densities connecting the FtsZ filaments laterally or diagonally (**Fig. 3a-c**, Supplementary Figs. 7a and 8a). Zoomed-in views of the toroids in the XY plane showed that the toroid consists of relatively short filament segments arranged nearly parallel to each other (**Fig. 3b** and Supplementary Fig. 8a). In contrast, cross-sectional views of the toroids revealed elongated structures rather than simple filament cross-sections along the Z-axis (**Fig. 3c** left, Supplementary Fig. 9a).

We then extracted the toroid isosurface from the tomograms to visualize its 3D structure (**Fig. 3c** right-e, Supplementary Fig. 8b-e and Supplementary video 1). The isosurface confirmed the presence of extended structures along the Z-axis, well beyond the elongation expected from the missing wedge effect for single FtsZ filaments (for comparison, see Supplementary Fig. 10). The vertically extended structures appeared to correspond to filaments that were connected or decorated by additional densities along the Z-axis (Supplementary Fig. 9b). Importantly, these densities were only observed in the presence of ZapD (Supplementary Fig. 10b), suggesting that they represent ZapD connections (**Fig. 3e** and Supplementary Figs. 8e and 9b). We note that the resolution of the data is not sufficient to precisely resolve ZapD proteins from the FtsZ filaments in the Z-axis.

These results suggest that the toroids are constructed and stabilized by interactions between ZapD and FtsZ, which are mainly formed along the Z-axis but also laterally and diagonally.

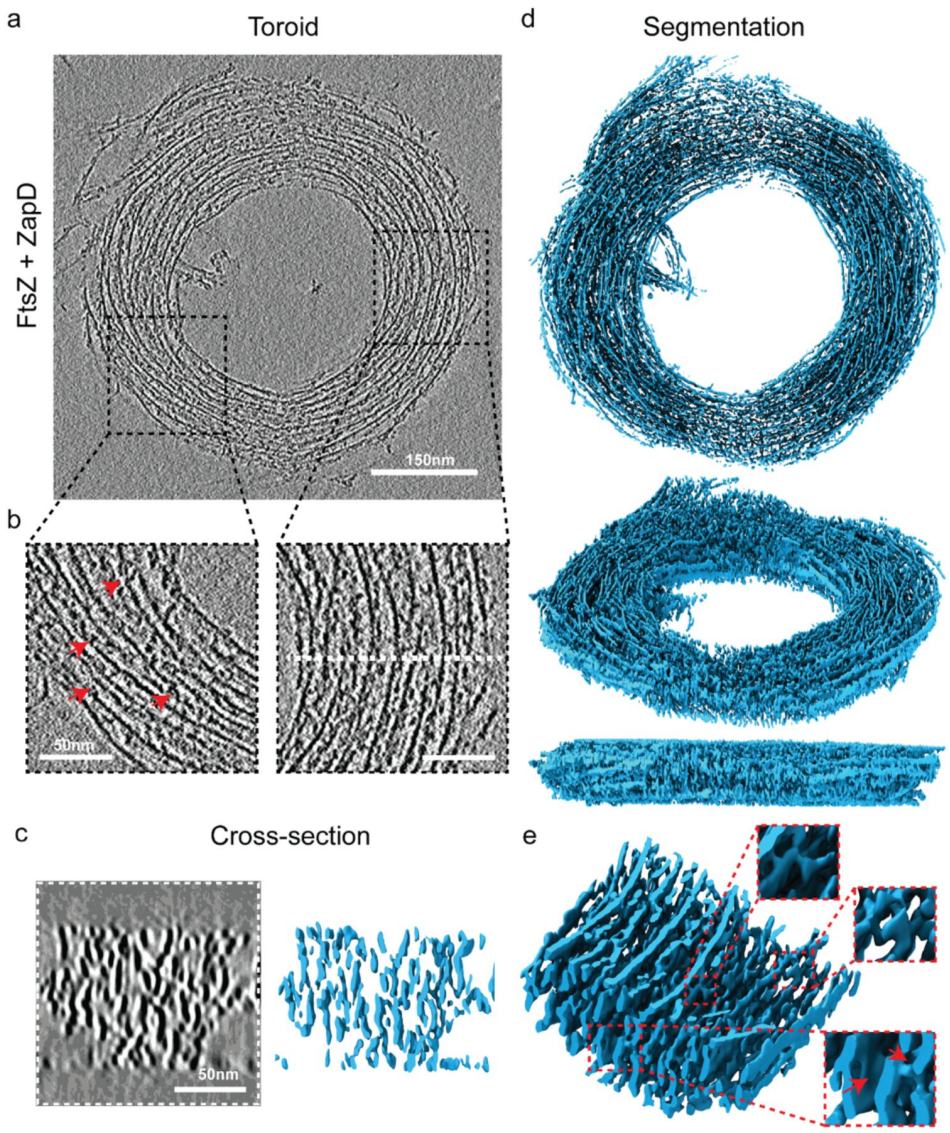

Figure 3.

3D structure of FtsZ toroids revealed by cryo-ET.

a. Representative tomographic slice of an FtsZ toroid resulting from the interaction of FtsZ with ZapD. The image is the average of five 0.86 nm thick tomographic slices (total thickness of 4.31 nm) of the reconstructed tomogram around the equatorial plane of a single FtsZ toroid. The concentrations of FtsZ and ZapD were 10 μM and 1 mM of GTP was added to initiate polymerization under working conditions (50 mM KCl, 50 mM Tris-Cl, 5 mM $MgCl_2$ pH 7).
b. Close-up views of the toroidal structure show the alignment of the FtsZ filaments forming the toroid. Red arrows indicate the presence of connections between filaments.
c. The tomographic slice in the XZ plane (left) shows the cross-section corresponding to the area marked by the white dotted line in **b.** This image is the average of nine tomographic slices (total thickness of 7.74 nm) from the denoised tomogram. The isosurface of the cross-section (right) shows the vertical alignment and stacking of the FtsZ filaments within the toroid. This suggests that the interaction between FtsZ filaments and ZapD is mainly along the Z direction. FtsZ filaments are represented in blue.
d. Isosurface of the FtsZ toroid shown in **a**. It was extracted from the reconstruction of the denoised tomographic volume and positioned in different views to facilitate its visualization: (top) front view, (middle) side view and (bottom) lateral view. The toroid has a diameter of ~552 nm and a height of ~92 nm.
e. A close-up view of the segmented toroidal structure. It shows the complex internal organization of filaments assembling the toroid. It corresponds to a zone within the toroid shown in **b** on the right. Close-up views of the isosurface show different connections between filaments. The segmentation shown has a width of 135.9 nm x 101.48 nm and a height of 63.64 nm.

ZapD plasticity is essential for toroid shape and stabilization

Next, we manually labeled the connecting densities in the toroid isosurfaces to analyze their arrangement and connectivity with the FtsZ filaments (**Fig. 4a**; Supplementary Movie 2). The high density of the toroids and the wide variety of conformations of these densities prevented the use of subtomogram averaging to resolve their structure and spatial arrangement within the toroids. Most connections exhibited a characteristic bi-spherical shape between the filaments, reminiscent of ZapD dimers (**Fig. 4b-d**). We observed lateral connections between two parallel FtsZ filaments at the same height within the toroid (**Fig. 4b**). In addition, FtsZ filaments at different heights can connect vertically and diagonally through ZapD proteins acting as bridging units, forming a complex 3D mesh (**Fig. 4c, d, and** Supplementary Movie 2). We also identified potential ZapD proteins that decorate individual FtsZ filaments and can link them to other nearby filaments (**Fig. 4b**). Furthermore, some filaments exhibited multiple crosslinks, leading to stronger attachments between them (**Fig. 4d**). Estimation of the precise number of ZapD molecules per FtsZ or the number of bonds per filament is challenging due to their inherently heterogeneous organization. However, we could observe a high number of connections stabilizing the toroidal structure. The short filament length, which results in gaps between adjacent filaments, does not correlate with a higher number of ZapD connections (Supplementary Fig. 11), indicating that ZapD is able to crosslink filaments in all directions without causing filament breakage. This could play an important mechanistic role in the functionality of the FtsZ macrostructures.

Cryo-ET imaging of ZapD-mediated FtsZ toroidal structures revealed a preferential vertical stacking and crosslinking of short ZapD filaments, which are also crosslinked laterally and diagonally, allowing for filament curvature and resulting in a toroidal structure observed for the first time following the interaction between FtsZ and one of its natural partners in vitro.

High concentrations of ZapD promote the structural reorganization of FtsZ polymers into straight bundles by tightly packed crosslinking from above

Having characterized the higher order FtsZ structures promoted at equimolar ZapD binding densities, we addressed the effect of increasing the ZapD density on the structural organization of the ZapD-FtsZ polymers. At high concentrations of ZapD (typically 40 – 60 μM, representing a molar ratio of approximately one to four or six to FtsZ), we observed the formation of straight bundles with striated patterns between the FtsZ filaments (Supplementary Fig. 12), as well as the presence of some toroidal structures (Supplementary Fig. 6a). Here, the high concentration of ZapD molecules increased the number of links between the filaments and ultimately promoted the formation of straight bundles, indicating that the assembly of FtsZ-ZapD structures is a reversible process that strongly depends on the amount of ZapD proteins crosslinking the filaments. Toroids and curved bundles always coexist, but the predominance shifts from toroids to straight bundles at high ZapD concentrations. This shift suggests that the number of crosslinks between filaments can modulate the properties of the assembled higher order structures, resulting in the reorganization of the toroidal structures into straight bundles upon ZapD saturation (Supplementary Fig. 12). We then explored how higher densities of ZapD lead to the formation of straight bundles using cryo-ET.

Using the same approach to visualize the toroids, we collected tomograms of the straight bundles and extracted their isosurfaces (**Fig. 5a**, Supplementary Fig. 7b, Supplementary Fig. 13 and Supplementary Movie 3). The straight bundles are formed at high ZapD concentrations and consist of a highly organized stack of well-aligned FtsZ filaments (**Fig. 5b**). The connection of filaments by multiple putative ZapD proteins results in the straightening of the structure of the filaments[10,50] (**Fig. 5c**). Interestingly, ZapD crosslink FtsZ filaments from the top, forming a

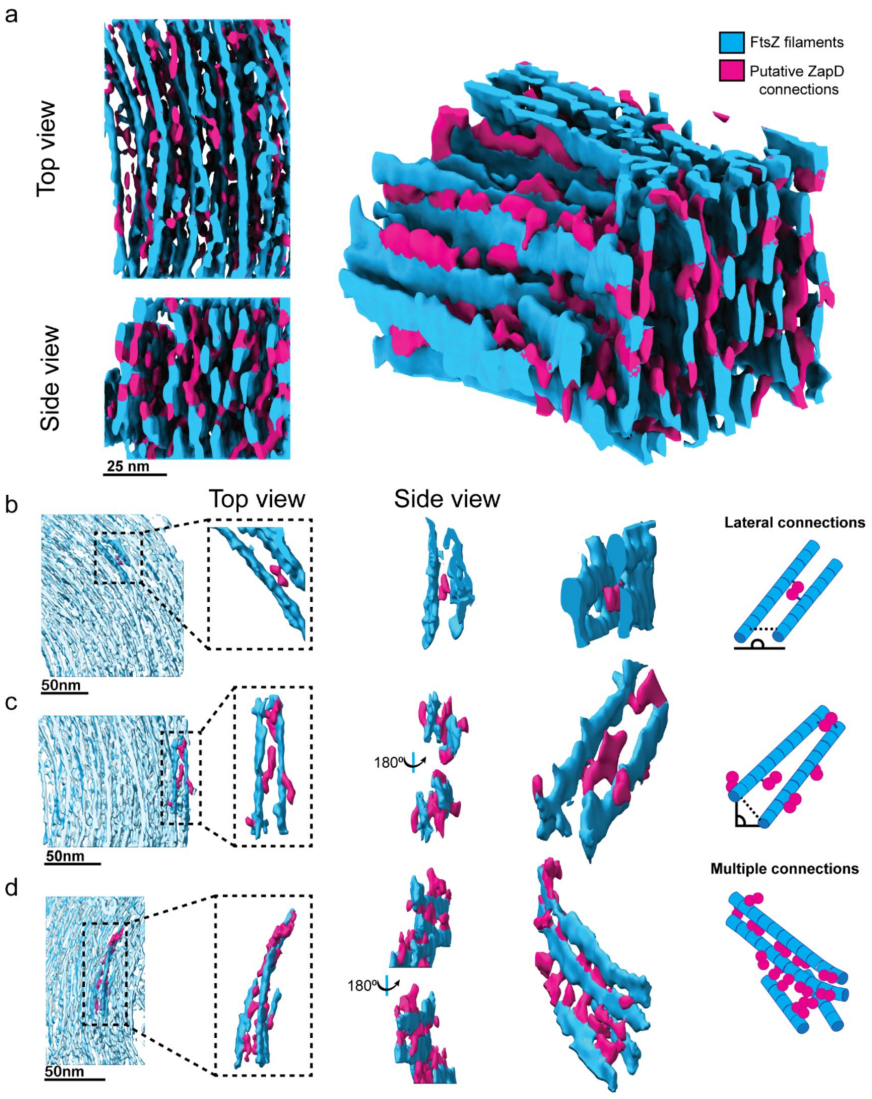

Figure 4.

FtsZ filaments are connected by putative ZapD crosslinkers to assemble the toroidal structure.

a. Top (left, top), side (left, bottom) and lateral (right) views of the isosurface from a region within the toroidal structure shown in **Fig. 3a**. The FtsZ filaments are colored in blue, while filament connections or putative ZapD proteins are labelled in magenta to facilitate interpretation of the results. Other putative ZapD proteins decorating the FtsZ filaments were not labelled in magenta because they were not forming any clear linkage between the filaments. The segmentation shown has a width of 73.1 nm x 101.48 nm and a height of 63.84 nm.
b-d Various examples of filament connections by putative ZapD proteins within the toroid. Same color code as in a. From left to right, the localization of the analyzed region, a close-up view of the structure of interest, different views of the crosslinkers and a schematic illustrating the interpretation of the data. The schematic (right) shows the localization of ZapD proteins (magenta) and FtsZ filaments (blue).
b. Lateral connection of two FtsZ filaments by a putative ZapD dimer. In this example, the attachment of each globular density or putative ZapD monomer was bound to each filament, allowing for lateral binding.
c. Putative ZapD connections stabilizing two filaments by a lateral interaction. Additional ZapD decorations attached to only one of the filaments appear to be available for other filament connections.
d. Multiple ZapD proteins can connect to filaments and stabilize the interaction. First, the two upper filaments are connected vertically by several putative ZapDs. The lower filament connects vertically in an oblique angle to the nearest neighboring filament. In the upper part, additional decorations or putative ZapD proteins would be available to establish further interactions forming a 3D mesh.

row of ZapD proteins interacting with both filaments (**Fig. 5d**). Here too, structural analysis by subtomogram averaging was not possible due to the crowding, preferential orientation, and heterogeneity of the connections. The distance between ZapD proteins provided a mean value of 4.5 ± 0.5 nm (Supplementary Fig. 14a), consistent with the size of FtsZ proteins[52]. This observation suggests that most FtsZ proteins interact with the ZapD dimers that crosslink the filaments, in agreement with the ZapD enrichment in the bundles observed by sedimentation assays (Supplementary Fig. 5). In addition, we found that the presence of ZapD increased the distance between two FtsZ filaments connected by ZapD proteins compared with the spacing in the absence of ZapD, regardless of the amount of ZapD connections (from 5.9 ± 0.8 nm to 7.88 ± 2 nm in toroids and 7.6 ± 1.5 nm in straight bundles; Supplementary Fig.14b). This indicates that ZapD not only connects neighboring FtsZ filaments but spreads them apart, which could have important implications for the functionality of the Z ring.

These results point out the relevant role of the number of connections between filaments (driven by ZapD binding) in the crosslinking mechanism (**Fig. 6**). The bundles formed at the high ZapD concentrations tested (up to four molar excess of ZapD to FtsZ) correspond to a binding saturation regime in which a ZapD dimer binds two FtsZ molecules connecting two filaments, straightening their structure and arranging them into large, highly organized straight bundles. In contrast, fewer connections provide the freedom to form toroidal structures. This observation confirms that a certain number of ZapD-driven bonds are optimal for maintaining the preferential curvature of FtsZ filaments and allowing toroid assembly, establishing a structural dependence of assembled bundles on the number of ZapD-mediated bonds.

Dimerization of ZapD is essential for the formation of organized higher-order FtsZ structures

Our results suggest that ZapD dimers connect two FtsZ filaments, although the role of dimerization has not yet been experimentally established[41]. We therefore investigated whether the dimerization of ZapD was essential for assembling straight bundles and toroidal structures. To this end, we produced a ZapD mutant (“mZapD”) by substituting three amino acids (R20, R116 and H140) involved in its dimerization by alanine, thus decreasing the stability of the dimerization interface. The dimerization of mZapD was tested by AUC analysis, which showed a percentage of monomeric protein that was not present in the wild-type ZapD (Supplementary Fig. 15a). mZapD can interact with unpolymerized FtsZ-GDP as evidenced by fluorescence anisotropy and FCS (Supplementary Fig. 15b and c). mZapD is still able to promote FtsZ bundle formation, showing a ~50% lower turbidity signal than for wild-type ZapD even at higher concentrations (Supplementary Fig. 15d). We also visualized these bundles by cryo-EM and observed the formation of thinner bundles (Supplementary Fig. 16b and c). However, toroidal structures and straight bundles were absent in these samples even at high concentrations of mZapD. This indicates that a stable dimerization interface is required to assemble complex ZapD-mediated structures (Supplementary Fig. 16a).

These results demonstrated that dimerization of ZapD is essential to promote the assembly of organized high-order FtsZ structures such as toroids and straight bundles, highlighting the structural importance of stable ZapD-driven connections between filaments.

Discussion

In this study, we used biochemical reconstitution, cryo-EM and cryo-ET to gain new insights into the structure and assembly of the bacterial divisome. Filament crosslinking by Zap proteins plays a crucial role in the assembly and stabilization of the Z ring. However, the underlying mechanisms

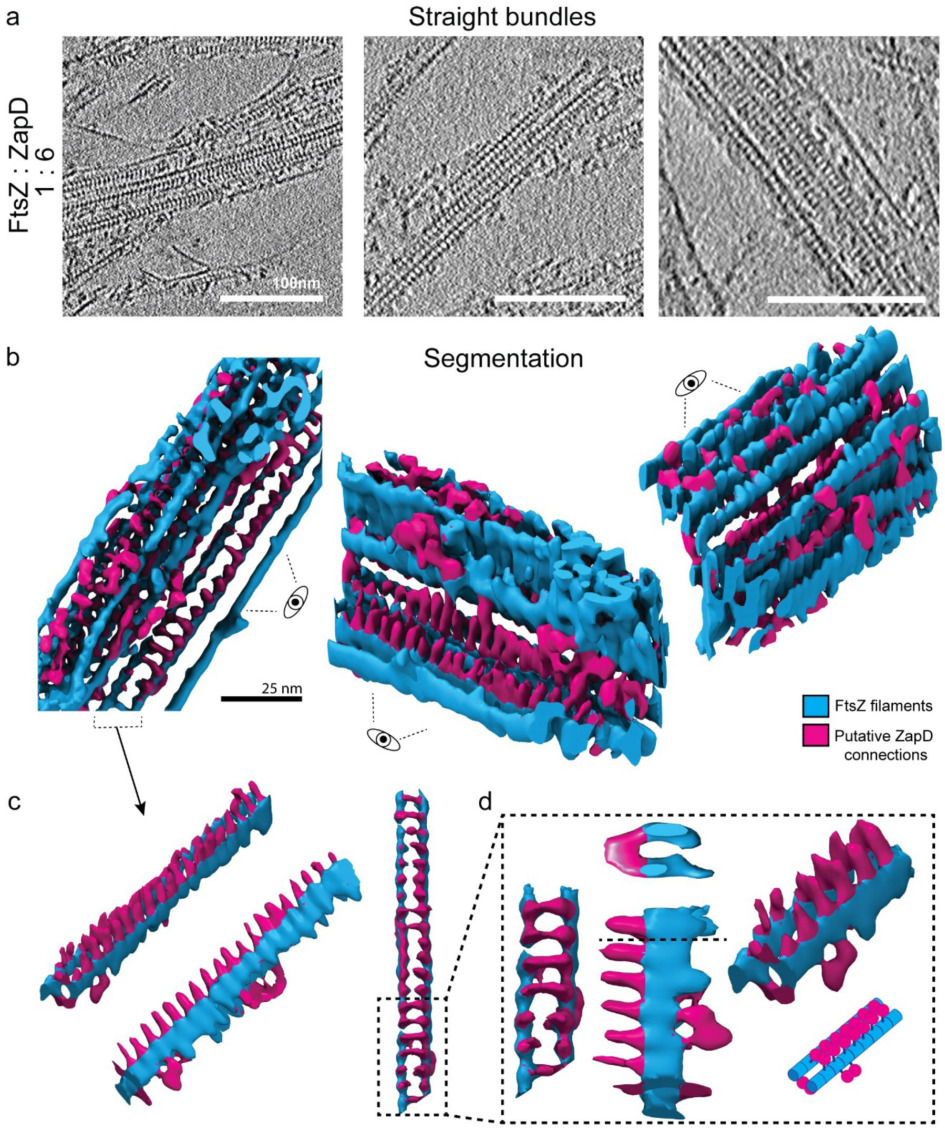

Figure 5.

Formation of straight FtsZ bundles is driven by high ZapD crosslinking from above.

a. Representative tomographic slices of straight FtsZ bundles resulting from the interaction of FtsZ with high ZapD concentrations under working conditions (50 mM KCl, 50 mM Tris-Cl, 5 mM $MgCl_2$ pH 7). The concentrations of FtsZ and ZapD were 10 μM and 60 μM, respectively, and 1 mM of GTP was added to trigger polymerization. The straight bundles were found only at high ZapD concentrations. The image is the average of five 0.86 nm thick tomographic slices (total thickness of 4.31 nm) of the reconstructed tomogram. Scale bars are 100 nm.
b. Isosurface of the straight bundles from the denoised tomographic volume. FtsZ filaments are colored in blue and putative ZapD connections in magenta. Three different views (top (left) and side views (middle, right)) are shown. Straight bundles are organized in a regular organization. Multiple bonds between filaments are formed from the top by putative ZapDs vertically crosslinking two FtsZ filaments with a regular spacing of 4.5 ± 0.5 nm between ZapD dimers. In addition, lateral connections were also found, connecting pairs of stabilized filaments to each other and eventually assembling the straight bundle.
c. Different views of one of the isolated filaments from the straight bundle. A side view of the filaments (middle) shows a spike-like structure regularly located at the top of the FtsZ filaments, connecting them vertically as observed in the top view (right).
d. Different close-up views of the filament structure shown in **c.** In the cross-section of the structure (middle, top), it is clearly visible that the ZapD proteins connect the two filaments vertically and from above, forming a bridge over them. A schematic of the proposed interaction (right, bottom) shows the position of putative ZapD dimers in this structure.

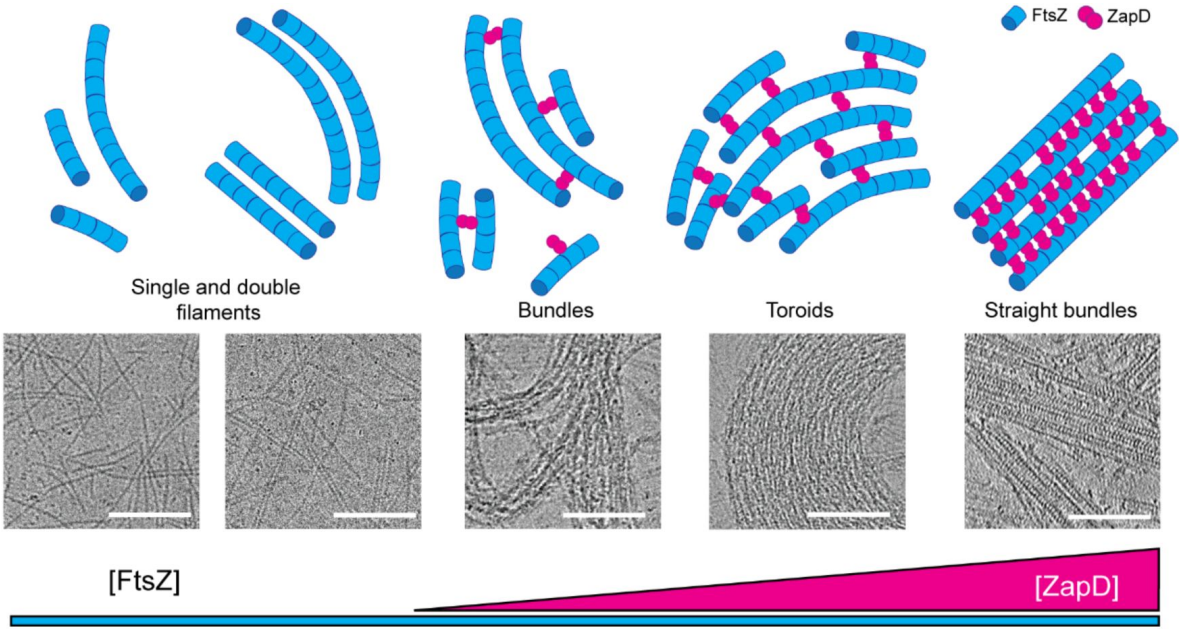

Figure 6.

The amount of ZapD connections modulates the spatial organization of FtsZ filaments into higher order structures.

(Top) Schematic of the higher order FtsZ structures formed in the presence of increasing concentrations of ZapD. (Bottom) Cryo-EM images of the structures shown in the schemes. In the absence of ZapD, FtsZ filaments can interact laterally to form double filaments upon GTP binding. At low concentrations of ZapD, only few ZapD-mediated bonds are formed, favoring the formation of small, curved bundles. At equimolar concentrations of ZapD and FtsZ, more ZapD-mediated bonds are formed, particularly from above the filaments, but also laterally and diagonally, allowing filament curvature and favoring the assembly of toroidal structures. At saturating ZapD concentrations, the filaments are straightened up by regular ZapD crosslinking from above, resulting in the formation of straight bundles. Overall, the assembly of higher order FtsZ structures depends on the number of vertical crosslinks through ZapD dimers. Some intermediate states are expected between the structures shown. Scale bars are 100 nm.

of this process remain to be elucidated. To better understand these mechanisms, we investigated the interaction between FtsZ and ZapD, one of the stabilizers of the division ring.

Our results indicate that ZapD crosslinks FtsZ in solution to form 3D toroidal structures characterized by short, discontinuous FtsZ filaments that are vertically stacked and crosslinked, as well as diagonally and laterally crosslinked, as revealed by cryo-ET. The relative concentrations of FtsZ and ZapD dictate the assembly geometry. Remarkably, FtsZ toroids emerge as the dominant structure when both proteins are present in equimolar ratios, whereas straight bundles are assembled at high concentrations of ZapD. Our study highlights the importance of the balance between vertical and lateral or diagonal crosslinking to allow for the filament curvature observed in the toroids, which is absent in the straight bundles where crosslinking from the top is dominant.

The structural characterization of the toroids by cryo-ET allowed us to resolve the overall structure and identify putative ZapD dimers that crosslink the filaments. However, we were unable to obtain detailed structural information about the ZapD connectors due to the heterogeneity and density of the toroidal structures, which showed significant variability in the conformations of the connections between the filaments in all directions. These results are consistent with the observation that ZapD interacts with FtsZ through its central hub, which provides additional spatial freedom to connect other filaments in different conformations. This flexibility allows different filament organizations and contributes to structural heterogeneity. In addition, these results suggest that these crosslinkers can act as modulators of the dynamics of the ring structure, spacing filaments apart and allowing them to slide in an organized manner[33,37,53,54]. The ability of FtsZ to treadmill directionally[34,55–58], together with the parallel or antiparallel arrangement of short, transiently crosslinked filaments, is considered essential for the functionality of the Z ring and its ability to exert constrictive force[34,36–38,50]. Thus, Zap proteins can play a critical role in ensuring correct filament placement and stabilization, which is consistent with the toroidal structure formed by ZapD.

Our observation of toroidal FtsZ structures promoted by ZapD in solution is consistent with the observation of pre-curved FtsZ protofilaments in circular assemblies attached to model membranes in various in vitro systems[55,56,59]. Additionally, FtsZ can form ring-shaped structures with diameters ranging from 100 to 200 nm on surfaces, becoming more pronounced when adsorbed to lipid, carbon, or mica surfaces[52,60,61], or in the presence of molecular crowders like methylcellulose[14]. Cryo-EM of concentrated (50 μM) FtsZ from *Bacillus subtilis* with GMPCPP revealed that these protofilaments often coalesce into spirals or toroids, forming large aggregates[31]. These toroidal structures correspond to the curved conformations of FtsZ polymers observed in various bacterial species, which are thought to contribute to the generation of constriction forces[50]. In *Escherichia coli*, approximately 5,000 FtsZ monomers (about one third of the intracellular concentration of FtsZ) could circle the cell 6-8 times[62], suggesting a discontinuous toroidal assembly. ZapD, present at approximately 500 molecules per cell[19], represents only a small fraction of the FtsZ molecules and favors the formation of toroidal structures in the absence of interactions with other FtsZ-associated proteins. Higher concentrations of ZapD would be required to form straight bundles.

The persistence length and curvature of FtsZ filaments are optimized to form bacterial-sized ring structures[7,50]. ZapD helps to stabilize these toroids by crosslinking and increasing the spacing between FtsZ filaments from 5.9 ± 0.8 nm to 7.9 ± 2 nm in toroids and 7.6 ± 1.5 nm in straight bundles (Supplementary Fig. 14b). This increased spacing promotes a more dynamic organization, providing functional flexibility in bacteria. The linker connecting ZapD to FtsZ can also modulate filament spacing and curvature[31,32,63]. We observe a mixture of curvatures in the internal organization of the toroids. While FtsZ filaments have a preferred curvature, the density of ZapD connections forces the structure to adapt and align with neighboring filaments, thereby affecting FtsZ curvature. However, the precise molecular mechanism linking ZapD binding and polymer curvature remains to be elucidated.

One of the most significant findings of this study is that the amount of ZapD bound to FtsZ filaments greatly influences the structural organization of the resulting higher order polymer. At lower concentrations of ZapD, which are necessary for bundling (equimolar mixtures of ZapD and FtsZ), toroids are the most prominent structures, containing one ZapD dimer for every four to six FtsZ molecules. When the concentration of ZapD increases, the density of ZapD binding in the polymers rises to one ZapD dimer for every two FtsZ molecules. This leads to a reorganization of the polymer bundles, resulting in straight structures that predominantly crosslink the FtsZ filaments, a configuration not seen at lower ZapD concentrations (**Fig. 5**). The increase in the number of ZapD-FtsZ contacts likely reduces the flexibility needed to form toroidal structures, compelling the filaments to adopt a larger, straight bundle conformation. We observed slight differences in the spacing between filaments (Supplementary Fig. 14b), with a broader range of distances between filaments in the toroids compared to the straight bundles. This makes sense, as ZapD is the molecule linking the filaments in both structures, although the amount of bound ZapD differs, allowing for greater variability in spacing within regions with a relatively fewer ZapD-FtsZ connections.

We therefore hypothesize that the assembly of functional, curved FtsZ macrostructures occurs only within a specific stoichiometric range of ZapD-FtsZ interactions. An increase in crosslinking at higher ZapD concentrations appears to cause the FtsZ polymer to form rigid, straight bundles (**Fig. 6**). Additionally, only a robust ZapD dimer can form FtsZ toroids and straight filaments, indicating that a certain binding strength is necessary to bundle the filaments and maintain their structure. These observations, along with the high conformational variability found in ZapD connections, suggest that ZapD can modulate the behavior of the entire structure through a concentration-dependent mechanism. This structural reorganization highlights the polymorphic nature of the assemblies formed by FtsZ[38,64].

We also demonstrated that ZapD-mediated FtsZ toroids replicate some of the structural features of the Z ring architecture observed in vivo. Based on super-resolution imaging and cryo-electron tomography (cryo-ET), the current model of the Z ring describes a somewhat discontinuous and heterogeneous structure composed of randomly overlapping filaments[33,45,65]. These filaments arrange into a belt-like macromolecular entity, containing nodes with a higher density of dispersed filaments confined to a toroidal zone approximately 80–100 nm wide (toroidal height) and about 40–60 nm thick, located 13-16 nm below the inner membrane[33,39,45,47,65–67]. The toroidal structures promoted by ZapD exhibit dimensions within this range. However, their thickness and multilayering are significantly greater, likely due to the absence of other cellular components competing for binding with FtsZ. The Z ring model also suggests that FtsZ filaments are weakly associated with one another through protein factors such as Zaps and weak FtsZ-FtsZ interactions, which may be crucial for their functionality[7,31,32,68]. Our findings indicate that one of the Zap proteins can stabilize and enhance associations between neighboring FtsZ filaments. Studying macrostructures stabilized by natural crosslinkers is vital for understanding the molecular function of the division machinery.

We believe that the intrinsic features of the toroidal structures share commonalities with the bacterial division ring. Despite the differences and limitations that may arise from an in vitro approach, the structures observed following ZapD crosslinking of FtsZ filaments may reveal inherent features that occur in vivo. The current model of the division ring consists of an array of filaments loosely connected by crosslinkers at the center of the cell, forming a ring. This model is consistent with our findings, although many questions remain regarding the structural organization of the Z ring within the cell. ZapD binds to FtsZ from above, allowing either ZapD or FtsZ to interact with the plasma membrane. In straight bundles, this facilitates the stacking of straight FtsZ filaments, while for toroids, ZapD can also bind FtsZ filaments diagonally. This less compact arrangement could allow bending of the FtsZ filaments and adjustment of the toroid size.

The binding of ZapA, a key member of the FtsZ-associated proteins family, to FtsZ in equimolar mixtures induces the effective alignment and straightening of FtsZ filaments tethered to lipid bilayers by FtsA protein, as demonstrated through high-resolution fluorescence microscopy and precise quantitative image analysis[69]. This interaction reveals a structure comprising one ZapA tetramer for every four FtsZ molecules in the polymer, highlighting the organized nature of these interactions. It is noteworthy that these straight, parallel polymers—manifested when ZapA occupies all binding sites—bear striking resemblance to the straight bundles identified in this study at high concentrations of ZapD, indicative of binding saturation. Understanding how the associative states of ZapA (as tetramers) and ZapD (as dimers), together with membrane tethering, influence the predominant structures formed in both systems is essential. The complexity of the division system raises important questions about the interaction dynamics between FtsZ and the plasma membrane. The competitive nature of the division components to engage with FtsZ and modulate its functionality remains to be thoroughly elucidated. It is important to note that FtsA and ZipA have a greater affinity for the C-terminal domain of FtsZ than ZapD. Our cryo-ET data on straight bundles provide new perspectives on how ZapD-FtsZ structures can effectively bind to the plasma membrane; in particular, the C-terminal domains of parallel FtsZ filaments are oriented upward, allowing direct membrane binding or interaction with ZapDs that reinforce these filaments from above, rather than from the side, as previously suggested[41].

In conclusion, this study extends the understanding of the intricate structural organization and filament crosslinking of FtsZ polymers facilitated by ZapD, which is critical for the formation and maintenance of the division ring. The revelation that ring morphology depends on the binding stoichiometry between FtsZ and the crosslinking ZapD is invaluable, particularly as we integrate this knowledge into current reconstitution assays in membrane systems. This knowledge is central to unraveling the role of FtsZ-associated proteins in coordinating and maintaining division ring formation. In addition, our findings could greatly enhance the understanding of how polymeric cytoskeletal networks are remodelled during essential cellular processes such as cell motility and morphogenesis. Although conventional wisdom points to molecular motors as the primary drivers of filament remodeling through energy consumption, there is increasing evidence that there are alternative mechanisms that do not rely on such energy, instead harnessing entropic forces via diffusible crosslinkers[70]. This approach may also be applicable to ZapD and FtsZ polymers, suggesting a promising avenue for optimizing conditions in the reverse engineering of the division ring to enhance force generation in minimally reconstituted systems aimed at achieving autonomous cell division.

Methods

Protein purification

ZapD protein has been overproduced and purified following the procedure previously described in[19] with some modifications. The bacterial strain was an *E. coli* BL21 (DE3) transformed with pET28b-h10-smt3-ZapD fusion plasmid[19]. The cells were sonicated for 6-8 cycles of 20 secs and centrifuged at 40.000 rpm in MLA 80 rotor (Beckman coulter) for 45 min. The protein was eluted by chromatography in 5-ml HisTrap (GE Healthcare) and digested with Smt3-specific protease Ulp1 (SUMO protease encoded in Rosetta pTB145), at 1:1 molar relation. Digestion proceeded for two dialysis of 1 hour at 4°C to avoid protein precipitation. ZapD and His-Smt3 were separated by chromatography in 5-ml HisTrap (GE Healthcare), then the protein was eluted in a 5-ml HiTrap Desalting column (Healtcare) to eliminate completely possible traces of free phosphates in the buffer. Final concentration of ZapD was determined by absorbance at 280 nm using an extinction coefficient (ε) of 25230 M^{-}

^{1} cm^{-1} and ZapD purity was checked by SDS-polyacrylamide gel electrophoresis. Protein fractions were frozen in buffer 50 mM KCL, 50 mM Tris-CL, 10 mM $MgCl_2$, 0.2 mM DTT and 2% glycerol. ZapD mutant (mZapD) was purified following the same procedure using the corresponding plasmid. *E. coli* FtsZ was overproduced and purified following the calcium precipitation method described previously[48]. Briefly, E. coli BL21 (DE3) pLysS cells were transformed with pET11b-FtsZ, grown in LB medium and selected with Ampicillin 100 µg/mL. After induction and growth, the pellet was resuspended in PEM buffer (50 mM PIPES-NaOH, pH 6.5, 5 mM $MgCl_2$, 1 mM EDTA) and disrupted using a tip sonicator for 3-4 cycles. The lysate was then separated by centrifugation for 30 min at 20,000 x g at 4 °C, and the supernatant was mixed with 1 mM GTP, 20 mM $CaCl_2$ and incubated at 30 °C for 15 min to induce FtsZ polymerization and bundling. Subsequently, the FtsZ bundles were pelleted by centrifugation for 15 min at 20,000 x g at 4 °C, and the pellet was resuspended in PEM buffer and centrifuged again for 15 min at 20,000 x g, 4 °C, collecting the supernatant. Precipitation and resuspension steps were repeated to improve the purification. The buffer was then exchanged using an Amicon Ultra-0.5 centrifugal filter unit 50 kDa (Merck KGaA). FtsZ purity was checked by SDS-polyacrylamide gel electrophoresis and concentration was determined by absorbance at 280 nm using an extinction coefficient (ε) of 14000 M^{-1} cm^{-1} [48]. Protein solutions were aliquoted, frozen in liquid nitrogen, and stored at –80 °C until further use.

Plasmid Design and Molecular Cloning

To generate the ZapD mutant (mZapD), seamless cloning method was used according to the provider's protocol (ThermoFisher Scientific /Invitrogen GeneArt™ Seamless Cloning and Assembly Enzyme Mix (A14606)) using the plasmid pET28b-h10-smt3-ZapD and the primers listed in (Supplementary Table 1). All enzymes for cloning were from Thermo Fisher Scientific (Waltham, MA, USA). Briefly, DNA fragments were amplified with Phusion High-Fidelity DNA Polymerase andorigo primers (Sigma–Aldrich, St. Louis, MO, USA). Then, PCR products were treated with DpnI and combined using GeneArt Seamless Cloning and Assembly Enzyme Mix. The plasmid was propagated in E. coli OneShot TOP10 (Thermo Fisher Scientific) and purified using NucleoBond Xtra Midi kit (Macherey-Nagel GmbH, Duren, Germany). Directed site mutagenesis was made by substituting three amino acids in the ZapD sequence by Alanine (R20, R116, H140). The plasmid was then verified using Sanger Sequencing Service (Microsynth AG, Balgach, Switzerland).

Protein labelling

Covalent labelling of FtsZ with Alexa 488 the amino groups of N-terminal amino acid residue with Alexa Fluor 488 carboxylic acid succinimidyl ester dye following the procedure previously described[13]. ZapD and mZapD were labelled with ATTO-647N carboxylic acid succinimidyl ester dye in the amino group. Before the reaction, ZapD was dialyzed in 20 mM HEPES, 50 mM KCl, 5 mM $MgCl_2$, pH 7.5 and the probe was dissolved in Dimethylsulfoxide (DMSO). The reaction was allowed to proceed for 35-60 min at RT and stopped with 10 % Tris-HCl 1 M. The free dye was separated from labelled protein by a Hi-TRAP Desalting column (GE Healthcare). The final degree of labelling of FtsZ and ZapD was calculated from the molar absorption coefficients of the protein and the dye. It was around 0.5 moles of probe per mole of FtsZ and around 0.3/0.4 moles of dye per mole of ZapD.

Analytical ultracentrifugation (AUC); sedimentation velocity (SV) and sedimentation equilibrium (SE)

Sedimentation velocity assays were performed to detect the homogeneity and association state of individual proteins and the stoichiometry of the formed protein-protein complexes. In brief, the experiments were carried out at 43-48 Krpm in an Optima XL-I analytical ultracentrifuge, equipped with UV–VIS absorbance and Raleigh interference detection systems. The sedimentation coefficient distributions were calculated by least-squares boundary modeling of sedimentation

velocity data using the c(s) method[71] as implemented in the SEDFIT program. The s-values of the present species were corrected to standard conditions (pure water at 20°C, and extrapolated to infinite dilution) to obtain the corresponding standard s-values (s20,w) using the program SEDNTERP[72]. Multi-signal sedimentation velocity (MSSV) data were globally analyzed by SEDPHAT software[73] using the "multi-wavelength discrete/continuous distribution analysis" model, to determine the spectral and diffusion deconvoluted sedimentation coefficient distributions, ck(s), from which the stoichiometry of protein complexes can be derived[74]. Sedimentation equilibrium of ZapD was carried out to confirm the association state of the protein in the same experimental conditions and concentration range tested by sedimentation velocity (2-30 μM). Short columns (100 μL) SE experiments were carried out at 14000 and 10000 rpm. Weight-average buoyant molecular weights were obtained by fitting a single-species model to the experimental data using the HeteroAnalysis program[75], once corrected for temperature and buffer composition with the program SEDNTERP[72].

Turbidity assay

Turbidity of protein samples was collected by measuring the absorbance at 350 nm in a TECAN plate reader (Tecan Group Ltd., Mannedorf, Switzerland). All samples reached a final volume of 50 μL in a 364-Well Flat-Bottom Microplate (UV-Star, Greiner Bio-One GmbH) before measuring the absorbance. Different concentrations of FtsZ and ZapD were premixed in the well-plate and measured before addition of GTP to extract subsequently the individual blank values. Concentrations of FtsZ and ZapD varied from 0 to 80 μM and buffer conditions are specified in each graph and the caption of the figures ranging from 50 to 500 mM KCl, 6 to 8 pH, always supplemented with 50 mM Tris-Cl and 5 mM $MgCl_2$. Manual mixing was performed after addition of GTP and orbital oscillations for 5 sec in the TECAN were made prior to any measurement to avoid sedimentation of the samples. FtsZ and ZapD alone do not generate significant differences with the blank. Time measurements were taken as specified in each condition. Reported values are the average of 3-12 independent measurements ± Standard deviation.

GTPase activity of FtsZ

GTPase activity of FtsZ was measured by quantification of the inorganic phosphate with a colorimetric assay (BIOMOL GREENÒ kit from ENZO life sciences) for two minutes. 5 μM FtsZ was used in our standard buffer (5 mM $MgCl_2$, 50 mM Tris-HCl, 50 mM KCl, pH 7) or buffers at higher KCl concentrations (50-500 mM KCl) and polymerization was triggered by 1 mM GTP. ZapD was added at different concentrations and premixed with FtsZ before addition of GTP. 13 μL fractions were added to a 96-Well Flat-Bottom Microplate (UV-Star, Greiner Bio-One GmbH) every 20 sec after addition of GTP and mixed with the Reaction buffer reaching 50 μL and 100 μL of BIOMOL GREEN reagent, to stop the reaction. After stopping the reaction, samples were incubated for 10 min at RT and the absorbance was measured at 620 nm in a Varioskan Flash plate reader (Thermo Fisher Scientific, MA, USA). Concentrations of inorganic Phosphate were calculated from a phosphate standard curve, while the GTPase activity reaction rate (V, mol P/mol FtsZ/ min) was determined from the slope of the linear part of phosphate accumulation curves.

FtsZ sedimentation assay

Purified ZapD (1-30 μM) was added to purified FtsZ (5 μM) in the working buffer (50 mM KCl, 50 mM Tris-HCl, 5 mM $MgCl_2$), and GDP or GTP (1 mM) was added last to trigger FtsZ polymerization. The reaction mixtures with a final volume of 100 μl were processed at room temperature and centrifuged at low speed (10.000 rcf) using a table top centrifuge. At that point, 90 μl of supernatant was carefully collected and loaded in clean tubes with 1x loading dye. The rest of the supernatant was discarded and the pellets were resuspended in the original reaction volume buffer plus 1× loading dye (final concentration). The supernatants (10 μl) and pellets (10 μl) were resolved in a SDS-PAGE gel. The amount of ZapD and FtsZ were estimated by image analysis using ImageJ.

Preparation of EM grids

Cryo-EM grids were plunge frozen with a Vitrobot Mk.IV (Thermo Fischer Scientific) using 3 µL of the samples applied to previously glow discharged R 2/1 Holey Carbon Cu 200 mesh EM grids (Quantifoil). Samples were 10 µM FtsZ with or without ZapD or mZapD at different concentrations specified in each case (0 – 60 µM). Proteins were mixed in our working buffer containing 50 mM, 5 mM $MgCl_2$, 50 mM Tris-HCl, pH 7. Samples were incubated for 2 minutes after the addition of 1 mM GTP to trigger polymerization. The Vitrobot was set to 4° C, 100% humidity, blot time 3 s, blot force 3. Whatman no. 1 filter paper was used for blotting and liquid ethane kept at liquid nitrogen temperatures was used as a cryogen for vitrification.

Cryo-EM and cryo-ET

Cryo-EM/ET data were acquired on two microscopes as follows. Cryo-EM micrographs were acquired within SerialEM[76] on a Talos Arctica transmission electron microscope (Thermo Fisher Scientific) operated at 200 kV, equipped with a Falcon III (Thermo Fisher Scientific) direct electron detector operated in integrating mode. Images were recorded at 73,000x magnification (pixel size 1.997 Å) and 92,000x magnification (pixel size 1.612 Å) at –2.5 µm to –5 µm target defocus with an approximate total electron dose of 60 electrons / Å². Cryo-EM micrographs and cryo-ET tilt series were acquired with SerialEM on a Titan Krios G2 transmission electron microscope (Thermo Fisher Scientific) operated at 300 kV, equipped with a FEG, post-column energy filter (Gatan) and a K3 camera (Gatan) operated in electron counting mode. Micrographs were recorded at 42,000x magnification (pixel size 2.154 Å) at – 5 µm target defocus with an approximate total electron dose of 60 electrons / Å². Tilt series were recorded at 42,000x magnification (pixel size 2.154 Å) at –5 µm target defocus with an approximate total electron dose of 100-140 electrons / Å². Acquisition was performed using a dose-symmetric tilt scheme, a tilt range of +/-60°, an angular increment of 2°.

Tomogram reconstruction

Tilt series preprocessing was performed using the TOMOMAN package (*https://github.com/williamnwan/TOMOMAN*). In brief, MotionCor2[77] was used to align individual frames, followed by cumulative dose-weighting using an exposure-dependent attenuation function, as described in[78]. Dose-weighted tilt series were aligned using IMOD[79] either by employing gold fiducials (if available) or by patch-tracking, and binned tomograms (pixel size 8.616 Å) were generated using weighted back-projection. Stacks were split into odd and even frames to generate half-set tomograms which were used for training and subsequent denoising in cryoCARE[80].

Denoised tomograms were used directly for segmentation of the toroids, straight bundles and individual filaments by cropping an area of interest and displaying the volume as an isosurface in USCF ChimeraX[81]. Thresholds for volume extraction were 80-100 and the color used were #00AEEF (light blue) for FtsZ and #EC008C (magenta) for ZapD isosurfaces. Small particles were removed by using the “dust” function with a size of 10. Different perspectives and zooms of the structures were manually adjusted for each figure in ChimeraX. To highlight connections between filaments, the corresponding parts with putative ZapD connections were manually cropped from the volume using the Volume Eraser tool in USCF Chimera[82]. Both cropped and original isosurfaces were superimposed to show the colored putative ZapDs in the structure. The missing wedge effect induces an elongation by a factor of 2 along the Z-axis. This elongation is observed in the filaments of the 1:0 ratio toroids, whereas the elongation observed in the filaments of the 1:1 and 1:6 ratio toroids exceeds the missing wedge.

All micrographs and slices through tomograms were visualized using IMOD. Isosurface renderings of toroids, straight bundles and individual filaments were displayed using USCF ChimeraX and USCF Chimera.

Fluorescence anisotropy

Anisotropy measurements were performed using a TECAN plate reader (Tecan Group Ltd., Mannedorf, Switzerland). Excitation and emission wavelengths were 625 nm and 680 nm, respectively. ZapD or mZapD labelled with ATTO 647N were used as fluorescence tracer with a final concentration of 150 nM of ATTO-647N and supplemented with unlabeled ZapD reaching a concentration of 5 μM. FtsZ was added at increasing concentrations to analyze their interaction. Binding affinities (apparent K_D) were determined by fitting the Hill equation to the normalized anisotropy data. Each condition was measured in three independent samples.

Fluorescence correlation spectroscopy (FCS)

FCS measurements were performed using a PicoQuant MicroTime200 system equipped with an Olympus 60x, NA1.2 UPlanApo water immersion objective. A pulsed 636 nm diode laser was used to excite fluorescence of Atto647N-labelled ZapD, mZapD or free Atto647N carboxylate (for calibration). Three measurements of 60 s each were performed per sample at room temperature (21°C), and three samples per condition were measured. The repetition rate of the pulsed laser was 26.7 MHz, and the average power was 1 μW at the objective back pupil. Fluorescence was collected through the same objective, spatially filtered through a 50 μm diameter pinhole, and spectrally filtered through a 690/70 nm bandpass filter before being split by a neutral beam splitter onto two avalanche photodiodes (Excelitas SPCM-AQRH-14-TR). Photon count events were digitized using a PicoQuant TimeHarp 260 Nano TCSPC card. Time-correlated single photon counting information was used for monitoring data quality during measurements, but not in further analysis. As especially in samples with FtsZ ZapD, and GTP present simultaneously we occasionally saw large, bright particles that are difficult to treat in FCS analysis, data was subjected to a burst removal algorithm similar to Margineanu et al. [83] and only “non-burst” data was used in correlation analysis to obtain statistics representative of the large number of small oligomer particles, ignoring rare large ones. Cross-correlation functions of the two detectors were calculated and fitted with a standard model for 3D diffusion in with rapid dye blinking:

$$G(\tau) = G_0\left[\frac{1 - F_B + F_B e^{-\frac{\tau}{\tau_B}}}{1 - F_B}\right]\frac{1}{1+\frac{\tau}{\tau_d}}\sqrt{\frac{1}{1+\frac{\tau}{S^2\tau_d}}}$$

With amplitude G_0, diffusion time τ_d, point spread function aspect ratio S, and blinking parameters F_B” and τ_B”. Custom software was written in Python for burst removal, correlation, and fitting, based on tttrlib 0.0.19 (*https://github.com/Fluorescence-Tools/tttrlib*). The software is in ongoing development, and available upon request.

Image analysis

Electron microscopy images were processed and analyzed using IMOD and ImageJ. The dimensions of the toroidal structures, FtsZ bundles and distances between filaments were manually measured using ImageJ and IMOD. Distances were plotted as histograms using Origin (OriginPro, Version *2019b*. OriginLab Corporation, Northampton, MA, USA.). For each toroid analyzed (n = 67) the inner and outer diameter were measured collecting the major and minor distance in each case. The circularity of the toroid was the result of the division between the minor diameter divided by major diameter for each toroid. The height of the FtsZ toroid was manually measured from the tomograms, collecting 4 measurements per toroid to assure a correct representation of the size (n = 17). For the spacing between filaments, the space in between the filaments was measured manually in the XY plane by using IMOD. Each measurement represents only one FtsZ double filament or one FtsZ-ZapD double filament, however, the same bundle could be measured more than once as they are composed for multiple filaments. The measurements were collected from >3 independent samples. The distances between ZapDs connecting two FtsZ

filaments were measured following the same methodology. The mean value and standard deviation of different datasets were calculated and added to the figures together with the n used for each case.

Acknowledgements

We thank Daniel Bollschweiller (MPIB cryo-EM facility) and Rafael Nuñez (CIB-CSIC imaging facility) for their help with the cryo-EM experiments. We also thank the MPIB core facility for assistance in protein purification, Michaela Schaper for plasmid cloning, Sigrid Bauer for lipid preparation and Noelia Ropero, Katharina Nakel and Kerstin Andersson for protein purification. We are also grateful to Miguel Robles-Ramos, Ana Raso, Hiromune Eto, Cristina Capitanio, Pedro Weickert, Kareem Al-Nahas, Yusuf Qutbuddin, Silvia Zorrilla, Henri Franquelim, Diego Ramirez and Daniela Garcia-Soriano for helpful discussions and fruitful input in this work. This work was funded by the Max Planck-Bristol Centre for Minimal Biology (A.M.-S.), the Deutsche Forschungsgemeinschaft (P.S.), the Deutsche Forschungsgemeinschaft (DFG) call ANR-DFG 2020 NLE through the grant JA-3038/2-1 (M. Ja.), the Germanýs Excellence Strategy – EXC-2094 – 390783311 (J.-H.K) and the Spanish Government through Grants PID2019-104544GB-I00 and PID2022_136951NB-I00 (G.R.). M.S.-S. was supported by European Social Fund through Grant PTA2020-018219-I. J.R.L.-O and M S.-S. acknowledge support from the Molecular Interactions Facility at the CIB Margarita Salas-CSIC. A.M.-S and J.-H.K. are part of IMPRS-LS, J.-H.K. is also a CeNS Center for NanoScience associate.

Additional information

Author contributions

Designing of research: A.M.-S., M.Ji., M.Ja., P.S. and G.R. Performing of research: A.M.-S, J.S., L.B., J.-H.K., M.S.-S., T.S., J.R.L.-O, C.A. and M.Ji. Data analysis: A.M.-S, J.S., T.S., J.R.L.-O, C.A., M.Ji., M.Ja. and G.R. Manuscript writing: A.M.-S (first draft); A.M.-S., M.Ja., P.S. and G.R. (final version); all authors revised and edited the manuscript, read the final version and approved to be published.

Additional files

Supplemental information

supplemental movie 1

supplemental movie 2

supplemental movie 3

References

1. Levin P. A., Janakiraman A. 2021) **Localization, Assembly, and Activation of the Escherichia coli Cell Division Machinery** *EcoSal Plus* **9**

2. Du S., Lutkenhaus J 2019) **At the Heart of Bacterial Cytokinesis: The Z Ring** *Trends Microbiol* **27**:781–791

3. Attaibi M., Den Blaauwen T 2022) **An Updated Model of the Divisome: Regulation of the Septal Peptidoglycan Synthesis Machinery by the Divisome** *Int. J. Mol. Sci* https://doi.org/10.3390/ijms23073537

4. Nogales E., Downing K. H., Amos L. A., Löwe J 1998) **Tubulin and FtsZ form a distinct family of GTPases** *Nat. Struct. Biol* **56**:451–458

5. De Boer P., Crossley R., Rothfield L 1992) **The essential bacterial cell-division protein FtsZ is a GTPase** *Nat. 1992 3596392* **359**:254–256

6. Addinall S. G., Lutkenhaus J 1996) **FtsA is localized to the septum in an FtsZ-dependent manner** *J. Bacteriol* **178**:7167–7172

7. McQuillen R., Xiao J 2020) **Insights into the Structure, Function, and Dynamics of the Bacterial Cytokinetic FtsZ-Ring** *Annu. Rev. Biophys* **49**:309–341

8. Wang M., Fang Chao, Ma B., Luo X., Hou Z. 2020) **Regulation of cytokinesis: FtsZ and its accessory proteins** *Curr. Genet* **66**:43–49

9. Wagstaff J. M., et al. 2017) **A Polymerization-Associated Structural Switch in FtsZ That Enables Treadmilling of Model Filaments** *MBio* **8**

10. Lu C., Reedy M., Erickson H. P 2000) **Straight and curved conformations of FtsZ are regulated by GTP hydrolysis** *J. Bacteriol* **182**:164–170

11. Mukherjee A., Lutkenhaus J 1999) **Analysis of FtsZ assembly by light scattering and determination of the role of divalent metal cations** *J. Bacteriol* **181**:823–832

12. Löwe J., Amos L. A 1999) **Tubulin-like protofilaments in Ca2+-induced FtsZ sheets** *EMBO J* **18**:2364–2371

13. González J. M., et al. 2003) **Essential cell division protein FtsZ assembles into one monomer-thick ribbons under conditions resembling the crowded intracellular environment** *J. Biol. Chem* **278**:37664–37671

14. Popp D., Iwasa M., Narita A., Erickson H. P., Maéda Y 2009) **FtsZ Condensates: An In Vitro Electron Microscopy Study** *Biopolymers* **91**:340–350

15. Squyres G. R., et al. 2021) **Single-molecule imaging reveals that Z-ring condensation is essential for cell division in Bacillus subtilis** *Nat. Microbiol* **6**:553–562

16. Ma X., Margolin W 1999) **Genetic and Functional Analyses of the Conserved C-Terminal Core Domain of Escherichia coli FtsZ** *J. Bacteriol* **181**:7531–7544

17. Hale C. A., De Boer P. A. J. 2002) **No Title** *J. Bacteriol* **184**:2552–2556

18. Wang X., Huang J., Mukherjee A., Cao C., Lutkenhaus J 1997) **Analysis of the interaction of FtsZ with itself, GTP, and FtsA** *J. Bacteriol* **179**:5551–5559

19. Durand-Heredia J., Rivkin E., Fan G., Morales J., Janakiraman A 2012) **Identification of ZapD as a cell division factor that promotes the assembly of FtsZ in Escherichia coli** *J. Bacteriol* **194**:3189–3198

20. Huang K.-H. H., Durand-Heredia J., Janakiraman A 2013) **FtsZ ring stability: Of bundles, tubules, crosslinks, and curves** *J. Bacteriol* **195**:1859–1868

21. Durand-Heredia J. M., Yu H. H., De Carlo S., Lesser C. F., Janakiraman A 2011) **Identification and characterization of ZapC, a stabilizer of the FtsZ ring in Escherichia coli** *J. Bacteriol* **193**:1405–1413

22. Ebersbach G., Galli E., Møller-Jensen J., Löwe J., Gerdes K 2008) **Novel coiled-coil cell division factor ZapB stimulates Z ring assembly and cell division** *Mol. Microbiol* **68**:720–735

23. de Boer P. A. J., Crossley R. E., Rothfield L. I 1989) **A division inhibitor and a topological specificity factor coded for by the minicell locus determine proper placement of the division septum in E. coli** *Cell* **56**:641–649

24. Tonthat N. K., et al. 2011) **Molecular mechanism by which the nucleoid occlusion factor, SlmA, keeps cytokinesis in check** *EMBO J* **30**:154–164

25. Ortiz C., Natale P., Cueto L., Vicente M 2016) **The keepers of the ring: regulators of FtsZ assembly** *FEMS Microbiol. Rev* **040**:57–67

26. Buske P. J., Levin P. A 2012) **Extreme C terminus of bacterial cytoskeletal protein FtsZ plays fundamental role in assembly independent of modulatory proteins** *J. Biol. Chem* **287**:10945–10957

27. Schumacher M. A., Zeng W., Huang K. H., Tchorzewski L., Janakiraman A 2016) **Structural and functional analyses reveal insights into the molecular properties of the Escherichia coli Z ring stabilizing protein, ZapC** *J. Biol. Chem* **291**:2485–2498

28. Huang K. H., Mychack A., Tchorzewski L., Janakiraman A 2016) **Characterization of the FtsZ C-Terminal variable (CTV) Region in Z-Ring assembly and interaction with the Z-Ring stabilizer ZapD in E. coli cytokinesis** *PLoS One* **11**:1–24

29. Choi H., Min K., Mikami B., Yoon H. J., Lee H. H 2016) **Structural and Biochemical Studies Reveal a Putative FtsZ Recognition Site on the Z-ring Stabilizer ZapD** *Mol. Cells* **39**:814–820

30. Roach E. J., et al. 2016) **Structure and mutational analyses of Escherichia coli ZapD reveal charged residues involved in FtsZ filament bundling** *J. Bacteriol* **198**:1683–1693

31. Huecas S., et al. 2017) **Self-Organization of FtsZ Polymers in Solution Reveals Spacer Role of the Disordered C-Terminal Tail** *Biophys. J* **113**:1831–1844

32. Sundararajan K., Goley E. D 2017) **The intrinsically disordered C-terminal linker of FtsZ regulates protofilament dynamics and superstructure in vitro** *J. Biol. Chem* **292**:20509–20527

33. Szwedziak P., Wang Q., Bharat T. A. M. M., Tsim M., Löwe J 2014) **Architecture of the ring formed by the tubulin homologue FtsZ in bacterial cell division** *eLife* **3**:e04601

34. Whitley K. D., et al. 2021) **FtsZ treadmilling is essential for Z-ring condensation and septal constriction initiation in Bacillus subtilis cell division** *Nat. Commun* **12**:1–13

35. S??derstr??m B., Daley D. O., Söderström B., Daniel, ..., Daley O. 2017) **The bacterial divisome: more than a ring?** *Curr. Genet* **63**:161–164

36. Erickson H. P., Anderson D. E., Osawa M 2010) **FtsZ in Bacterial Cytokinesis: Cytoskeleton and Force Generator All in One** *Microbiol. Mol. Biol. Rev* **74**:504–528

37. Nguyen L. T., Oikonomou C. M., Jensen G. J 2021) **Simulations of Proposed Mechanisms of FtsZ-Driven Cell Constriction** *J. Bacteriol* **203**

38. Mateos-Gil P., Tarazona P., 'Elez M. V., Vélez M. 2019) **Bacterial cell division: modeling FtsZ assembly and force generation from single filament experimental data** *FEMS Microbiol. Rev* **039**:73–87

39. Buss J., et al. 2013) **In vivo organization of the FtsZ-ring by ZapA and ZapB revealed by quantitative super-resolution microscopy** *Mol. Microbiol* **89**:1099–1120

40. Hale C. A., et al. 2011) **Identification of Escherichia coli ZapC (YcbW) as a component of the division apparatus that binds and bundles FtsZ polymers** *J. Bacteriol* **193**:1393–1404

41. Schumacher M. A., Huang K. H., Zeng W., Janakiraman A 2017) **Structure of the z ring-associated protein, zapd, bound to the c-terminal domain of the tubulin-like protein, ftsz, suggests mechanism of z ring stabilization through ftsz cross-linking** *J. Biol. Chem* **292**:3740–3750

42. Pazos M., Natale P., Margolin W., Vicente M 2013) **Interactions among the early Escherichia coli divisome proteins revealed by bimolecular fluorescence complementation** *Environ. Microbiol* **15**:3282–3291

43. Bailey M. W., Bisicchia P., Warren B. T., Sherratt D. J., Männik J 2014) **Evidence for Divisome Localization Mechanisms Independent of the Min System and SlmA in Escherichia coli** *PLOS Genet* **10**:e1004504

44. Gong H., et al. 2024) **The divisome is a self-enhancing machine in Escherichia coli and Caulobacter crescentus** *Nat. Commun* **151**:1–19

45. Fu G., et al. 2010) **In Vivo Structure of the E. coli FtsZ-ring Revealed by Photoactivated Localization Microscopy (PALM)** *PLoS One* **5**:e12680

46. Li Z., Trimble M. J., Brun Y. V., Jensen G. J 2007) **The structure of FtsZ filaments in vivo suggests a force-generating role in cell division** *EMBO J* **26**:4694–4708

47. Lyu Z., Coltharp C., Yang X., Xiao J 2016) **Influence of FtsZ GTPase activity and concentration on nanoscale Z-ring structure in vivo revealed by three-dimensional Superresolution imaging** *Biopolymers* **105**:725–734

48. Rivas G., et al. 2000) **Magnesium-induced linear self-association of the FtsZ bacterial cell division protein monomer. The primary steps for FtsZ assembly** *J. Biol. Chem* https://doi.org/10.1074/jbc.275.16.11740

49. Kourkoutis L. F., Plitzko J. M., Baumeister W 2012) **Electron Microscopy of Biological Materials at the Nanometer Scale** *Annual Review of Material Research* **42**:33–58 https://doi.org/10.1146/annurev-matsci-070511-155004

50. Erickson H. P., Osawa M 2017) **FtsZ Constriction Force-Curved Protofilaments Bending Membranes** *Subcell. Biochem* **84**

51. Wang N., et al. 2019) **Assembly properties of the bacterial tubulin homolog FtsZ from the cyanobacterium synechocystis sp. PCC 6803** *J. Biol. Chem* **294**:16309–16319

52. Huecas S., et al. 2007) **The interactions of cell division protein FtsZ with guanine nucleotides** *J. Biol. Chem* **282**:37515–37528

53. Lan G., Daniels B. R., Dobrowsky T. M., Wirtz D., Sun S. X 2009) **Condensation of FtsZ filaments can drive bacterial cell division** *Proc. Natl. Acad. Sci. U. S. A* **106**:121–126

54. Hörger I., Velasco E., Rivas G., Vélez M., Tarazona P 2008) **FtsZ Bacterial Cytoskeletal Polymers on Curved Surfaces: The Importance of Lateral Interactions** *Biophys. J* **94**:L81–L83

55. Loose M., Mitchison T. J 2014) **The bacterial cell division proteins FtsA and FtsZ self-organize into dynamic cytoskeletal patterns** *Nat. Cell Biol* **16**

56. Ramirez-Diaz D. A., et al. 2018) **Treadmilling analysis reveals new insights into dynamic FtsZ ring architecture** *PLOS Biol* **16**:e2004845

57. Yang X., et al. 2017) **GTPase activity-coupled treadmilling of the bacterial tubulin FtsZ organizes septal cell wall synthesis** *Science (80-.)* **355**:744–747

58. Bisson-Filho A. W., et al. 2017) **Treadmilling by FtsZ filaments drives peptidoglycan synthesis and bacterial cell division** *Science (80-.)* **355**:739–743

59. Boutte C. C., Srinivasan R., Sass P., Vélez M 2022) **How Does the Spatial Confinement of FtsZ to a Membrane Surface Affect Its Polymerization Properties and Function?** *Front. Microbiol* **13**:757711

60. Mingorance J., et al. 2005) **Visualization of single Escherichia coli FtsZ filament dynamics with atomic force microscopy** *J. Biol. Chem* **280**:20909–20914

61. González J. M., et al. 2005) **Cooperative behavior of Escherichia coli cell-division protein FtsZ assembly involves the preferential cyclization of long single-stranded fibrils** *Proc. Natl. Acad. Sci* **102**:1895–1900

62. Stricker J., Maddox P., Salmon E. D., Erickson H. P 2002) **Rapid assembly dynamics of the Escherichia coli FtsZ-ring demonstrated by fluorescence recovery after photobleaching** *Proc. Natl. Acad. Sci* **99**:3171–3175

63. Sundararajan K., Vecchiarelli A., Mizuuchi K., Goley E. D 2018) **Species– and C-terminal linker-dependent variations in the dynamic behavior of FtsZ on membranes in vitro** *Mol. Microbiol* **110**:47–63

64. Monterroso B., Alfonso C., Zorrilla S., Rivas G. 2013) **Combined analytical ultracentrifugation, light scattering and fluorescence spectroscopy studies on the functional associations of the bacterial division FtsZ protein. Methods** Academic Press Inc. pp. 349–362

65. Rowlett V. W., Margolin W 2014) **3D-SIM Super-resolution of FtsZ and Its Membrane Tethers in Escherichia coli Cells** *Biophys. J* **107**:L17–L20

66. Holden S. J., et al. 2014) **High throughput 3D super-resolution microscopy reveals Caulobacter crescentus in vivo Z-ring organization** *Proc. Natl. Acad. Sci. U. S. A* **111**:4566–4571

67. Szwedziak P., Ghosal D 2017) **FtsZ-ring architecture and its control by MinCD** *Subcell. Biochem* **84**:213–244

68. Haeusser D. P., Rowlett V. W., Margolin W 2015) **A mutation in Escherichia coli ftsZ bypasses the requirement for the essential division gene zipA and confers resistance to FtsZ assembly inhibitors by stabilizing protofilament bundling** *Mol. Microbiol* **97**:988–1005

69. Caldas P., et al. 2019) **Cooperative ordering of treadmilling filaments in cytoskeletal networks of FtsZ and its crosslinker ZapA** *Nat. Commun* **101**:1–13

70. Braun M., Lansky Z., Hilitski F., Dogic Z., Diez S 2016) **Entropic forces drive contraction of cytoskeletal networks** *BioEssays* **38**:474–481

71. Schuck P 2000) **Size-distribution analysis of macromolecules by sedimentation velocity ultracentrifugation and lamm equation modeling** *Biophys. J* **78**:1606–1619

72. Laue T. M., Shah B. D., Ridgeway T. M., Pelletier S. L 1992) **Analytical ultracentrifugation in biochemistry and polymer science** *Analytical ultracentrifugation in biochemistry and polymer science (Royal Society of Chemistry*

73. Schuck P 2003) **On the analysis of protein self-association by sedimentation velocity analytical ultracentrifugation** *Anal. Biochem* **320**:104–124

74. Balbo A., et al. 2005) **Studying multiprotein complexes by multisignal sedimentation velocity analytical ultracentrifugation** *Proc. Natl. Acad. Sci. U. S. A* **102**:81–86

75. Cole J. L 2004) **Analysis of Heterogeneous Interactions** *Methods Enzymol* **384**:212–232

76. Mastronarde D. N 2005) **Automated electron microscope tomography using robust prediction of specimen movements** *J. Struct. Biol* **152**:36–51

77. Zheng S. Q., et al. 2017) **MotionCor2: anisotropic correction of beam-induced motion for improved cryo-electron microscopy** *Nat. Methods* **144**:331–332

78. Schur F. K. M., et al. 2016) **An atomic model of HIV-1 capsid-SP1 reveals structures regulating assembly and maturation** *Science (80-.)* **353**:506–508

79. Kremer J. R., Mastronarde D. N., McIntosh J. R 1996) **Computer Visualization of Three-Dimensional Image Data Using IMOD** *J. Struct. Biol* **116**:71–76

80. Buchholz T. O., Jordan M., Pigino G., Jug F 2019) **Cryo-CARE: Content-aware image restoration for cryo-transmission electron microscopy data** *Proc. – Int. Symp. Biomed. Imaging* :502–506

81. Goddard T. D., et al. 2018) **UCSF ChimeraX: Meeting modern challenges in visualization and analysis** *Protein Sci* **27**:14–25

82. Pettersen E. F., et al. 2004) **UCSF Chimera—A visualization system for exploratory research and analysis** *J. Comput. Chem* **25**:1605–1612

83. Margineanu A., et al. 2007) **Complexation of Lipofectamine and Cholesterol-Modified DNA Sequences Studied by Single-Molecule Fluorescence Techniques** *Biomacromolecules* https://doi.org/10.1021/bm700486q

Author information

Adrián Merino-Salomón
Department of Cellular and Molecular Biophysics, Max Planck Institute of Biochemistry, Martinsried, Germany
ORCID iD: 0000-0002-6132-5314

Jonathan Schneider
Department of Molecular Structural Biology, Max Planck Institute of Biochemistry, Martinsried, Germany

Leon Babl
Department of Cellular and Molecular Biophysics, Max Planck Institute of Biochemistry, Martinsried, Germany
ORCID iD: 0000-0003-3279-8910

Jan-Hagen Krohn
Department of Cellular and Molecular Biophysics, Max Planck Institute of Biochemistry, Martinsried, Germany, Exzellenzcluster ORIGINS, Boltzmannstr. Garching, Germany

Marta Sobrinos-Sanguino
Molecular Interactions Facility, Centro de Investigaciones Biológicas Margarita Salas, Consejo Superior de Investigaciones Científicas (CSIC), Madrid, Spain

Tillman Schäfer
Cryo-EM facility, Max Planck Institute of Biochemistry, Martinsried, Germany

Juan R Luque-Ortega
Molecular Interactions Facility, Centro de Investigaciones Biológicas Margarita Salas, Consejo Superior de Investigaciones Científicas (CSIC), Madrid, Spain

Carlos Alfonso
Centro de Investigaciones Biológicas Margarita Salas, Consejo Superior de Investigaciones Científicas (CSIC), Madrid, Spain

Mercedes Jiménez
Centro de Investigaciones Biológicas Margarita Salas, Consejo Superior de Investigaciones Científicas (CSIC), Madrid, Spain

Marion Jasnin
Helmholtz Pioneer Campus, Helmholtz Munich, Germany; Department of Chemistry, Technical University of Munich, Garching, Germany
ORCID iD: 0000-0003-1726-4566

For correspondence: marion.jasnin@helmholtz-munich.de

Petra Schwille
Department of Cellular and Molecular Biophysics, Max Planck Institute of Biochemistry, Martinsried, Germany
ORCID iD: 0000-0002-6106-4847

For correspondence: schwille@biochem.mpg.de

Germán Rivas
Centro de Investigaciones Biológicas Margarita Salas, Consejo Superior de Investigaciones Científicas (CSIC), Madrid, Spain
ORCID iD: 0000-0003-3450-7478

For correspondence: rivas@cib.csic.es

Editors

Reviewing Editor
Mohan Balasubramanian
University of Warwick, Coventry, United Kingdom

Senior Editor
Felix Campelo
Institute of Photonic Sciences, Barcelona, Spain

Reviewer #1 (Public review):

Summary:

The major result in the manuscript is the observation of the higher order structures in a cryoET reconstruction that could be used for understanding the assembly of toroid structures. The cross-linking ability of ZapD dimers result in bending of FtsZ filaments to a constant curvature. Many such short filaments are stitched together to form a toroid like structure. The geometry of assembly of filaments - whether they form straight bundles or toroid like structures - depends on the relative concentrations of FtsZ and ZapD.

Strengths:

In addition to a clear picture of the FtsZ assembly into ring-like structures, the authors have carried out basic biochemistry and biophysical techniques to assay the GTPase activity, the kinetics of assembly, and the ZapD to FtsZ ratio.

Weaknesses:

The discussion does not provide an overall perspective that correlates the cryoET structural organisation of filaments with the biophysical data. The current version has improved in

terms of addressing this weakness and clearly states the lacuna in the model proposed based on the technical limitations.

Future scope of work includes the molecular basis of curvature generation and how molecular features of FtsZ and ZapD affect the membrane binding of the higher order assembly.

https://doi.org/10.7554/eLife.95557.2.sa2

Reviewer #3 (Public review):

Summary:

Previous studies have analyzed the binding of ZapD to FtsZ and provided images of negatively stained toroids and straight bundles, where FtsZ filaments are presumably crosslinked by ZapD dimers. Toroids without ZapD have also been previously formed by treating FtsZ with crowding agents. The present study is the first to apply cryoEM tomography, which can resolve the structure of the toroids in 3D. This shows a complex mixture of filaments and sheets irregularly stacked in the Z direction and spaced radially. The most important interpretation would be to distinguish FtsZ filaments from ZapD crosslinks, This is less convincing. The authors seem aware of the ambiguity: "However, we were unable to obtain detailed structural information about the ZapD connectors due to the heterogeneity and density of the toroidal structures, which showed significant variability in the conformations of the connections between the filaments in all directions." Therefore, the reader may assume that the crosslinks identified and colored red are only suggestions, and look for their own structural interpretations. But readers should also note some inconsistencies in stoichiometry and crosslinking arrangements that are detailed under "weaknesses."

Strengths.

This is the first cryoEM tomography to image toroids and straight bundles of FtsZ filaments bound to ZapD. A strength is the resolution, which. at least for the straight bundles. is sufficient to resolve the ~4.5 nm spacing of ZapD dimers attached to and projecting subunits of an FtsZ filament. Another strength is the pelleting assay to determine the stoichiometry of ZapD:FtsZ (although this also leads to weaknesses of interpretation).

Weaknesses

The stoichiometry presents some problems. Fig. S5 uses pelleting to convincingly establish the stoichiometry of ZapD:FtsZ. Although ZapD is a dimer, the concentration of ZapD is always expressed as that of its subunit monomers. Fig. S5 shows the stoichiometry of ZapD:FtsZ to be 1:1 or 2:1 at equimolar or high concentrations of ZapD. Thus at equimolar ZapD, each ZapD dimer should bridge two FtsZ's, likely forming crosslinks between filaments. At high ZapD, each FtsZ should have it's own ZapD dimer. However, this seems contradicted by later statements in Discussion and Results. (1) "At lower concentrations of ZapD, .. toroids are the most prominent structures, containing one ZapD dimer for every four to six FtsZ molecules." Shouldn't it be one ZapD dimer for every two FtsZ? (2) "at the high ZapD concentration...a ZapD dimer binds two FtsZ molecules connecting two filaments." Doesn't Fig. S5 show that each FtsZ subunit has its own ZapD dimer? And wouldn't this saturate the CTD sites with dimers and thus minimize crosslinking?

A major weakness is the interpretation of the cryoEM tomograms, specifically distinguishing ZapD from FtsZ. The distinction of crosslinks seems based primarily on structure: long continuous filaments (which often appear as sheets) are FtsZ, and small masses between filaments are ZapD. The density of crosslinks seems to vary substantially over different parts

of the figures. More important, the density of ZapD's identified and colored red seem much lower than the stoichiometry detailed above. Since the mass of the ZapD monomer is half that of FtsZ, the 1:1 stoichiometry in toroids means that 1/3 of the mass should be ZapD and 2/3 FtsZ. However, the connections identified as ZapD seem much fewer than the expected 1/3 of the mass. The authors conclude that connections run horizontally, diagonally and vertically, which implies no regularity. This seems likely, but as I would suggest that readers need to consider for themselves what they would identify as a crosslink.

In contrast to the toroids formed at equimolar FtsZ and ZapD, thin bundles of straight filaments are assembled in excess ZapD. Here the stoichiometry is 2:1, which would mean that every FtsZ should have a bound ZapD DIMER. The segmentation of a single filament in Fig. 5e seems to agree with this, showing an FtsZ filament with spikes emanating like a picket fence, with a 4.5 nm periodicity. This is consistent with each spike being a ZapD dimer, and every FtsZ subunit along the filament having a bound ZapD dimer. But if each FtsZ has its own dimer, this would seem to eliminate crosslinking. The interpretative diagram in Fig. 6, far right, which shows almost all ZapD dimers bridging two FtsZs on opposite filaments, would be inconsistent with this 2:1 stoichiometry.

In the original review I suggested a control that might help identify the structures of ZapD in the toroids. Popp et al (Biopolymers 2009) generated FtsZ toroids that were identical in size and shape to those here, but lacking ZapD. These toroids of pure FtsZ were generated by adding 8% polyvinyl chloride, a crowding agent. The filamentous substructure of these toroids in negative stain seemed very similar to that of the ZapD toroids here. CryoET of these toroids lacking ZapD might have been helpful in confirming the identification of ZapD crosslinks in the present toroids. However, the authors declined to explore this control.

Finally, it should be noted that the CTD binding sites for ZapD should be on the outside of curved filaments, the side facing the membrane in the cell. All bound ZapD should project radially outward, and if it contacted the back side of the next filament, it should not bind (because the CTD is on the front side). The diagram second to right in Fig. 6 seems to incorporate this abortive contact.

https://doi.org/10.7554/eLife.95557.2.sa1

Author response:

The following is the authors' response to the original reviews.

> ***Public Reviews:***
>
> ***Reviewer #1 (Public Review):***
>
> *Summary:*
>
> *The major result in the manuscript is the observation of the higher order structures in a cryoET reconstruction that could be used for understanding the assembly of toroid structures. The crosslinking ability of ZapD dimers result in bending of FtsZ filaments to a constant curvature. Many such short filaments are stitched together to form a toroid like structure. The geometry of assembly of filaments - whether they form straight bundles or toroid like structures - depends on the relative concentrations of FtsZ and ZapD.*
>
> *Strengths:*
>
> *In addition to a clear picture of the FtsZ assembly into ring-like structures, the authors have carried out basic biochemistry and biophysical techniques to assay the GTPase activity, the kinetics of assembly, and the ZapD to FtsZ ratio.*

> *Weaknesses:*
>
> *The discussion does not provide an overall perspective that correlates the cryoET structural organisation of filaments with the biophysical data.*
>
> *The crosslinking nature of ZapD is already established in the field. The work carried out is important to understand the ring assembly of FtsZ. However, the availability of the cryoET observations can be further analysed in detail to derive many measurements that will help validate the model, and obtain new insights.*

We thank the reviewer for these insightful comments on our work. We have edited the manuscript to resolve and clarify most of the issues raised during the review process.

> ***Reviewer #2 (Public Review):***
>
> *Summary:*
>
> *In this paper, the authors set out to better understand the mechanism by which the FtsZ-associated protein ZapD crosslinks FtsZ filaments to assemble a large-scale cytoskeletal assembly. For this aim, they use purified proteins in solution and a combination of biochemical, biophysical experiments and cryo-EM. The most significant finding of this study is the observation of FtsZ toroids that form at equimolar concentrations of the two proteins.*
>
> *Strengths:*
>
> *Many experiments in this paper confirm previous knowledge about ZapD. For example, it shows that ZapD promotes the assembly of FtsZ polymers, that ZapD bundles FtsZ filaments, that ZapD forms dimers and that it reduces FtsZ's GTPase activity. The most novel discovery is the observation of different assemblies as a function of ZapD:FtsZ ratio. In addition, using CryoEM to describe the structure of toroids and bundles, the paper provides some information about the orientation of ZapD in relation to FtsZ filaments. For example, they found that the organization of ZapD in relation to FtsZ filaments is "intrinsic heterogeneous" and that FtsZ filaments were crosslinked by ZapD dimers pointing in all directions. The authors conclude that it is this plasticity that allows for the formation of toroids and its stabilization. Unfortunately, a high-resolution structure of the protein organization was not possible. These are interesting findings that in principle deserve publication.*

We thank the reviewer for this valuable assessment. We have made several changes to the manuscript to improve its readability and comprehensibility. In addition, we have addressed the reviewer's main concerns in the point-by-point response below.

> *Weaknesses:*
>
> *While the data is convincing, their interpretation has some substantial weaknesses that the authors should address for the final version of this paper.*

We have addressed most of the aspects highlighted by the reviewer to improve the quality and comprehensibility of our results.

> *For example, as the authors are the first to describe FtsZ-ZapD toroids, a discussion why this has not been observed in previous studies would be very interesting, i.e. is it due to buffer conditions, sample preparation?*

Several factors may explain the absence of observed toroidal structures in other studies. FtsZ is a highly dynamic protein, and its behavior varies significantly with different environmental conditions, as detailed in the literature. These environmental factors include pH, salt concentration, protein type, GTP levels, and the purification strategy used. Previous research has employed negative stain electron microscopy (EM) to visualize ZapD-FtsZ structures. It is important to note that FtsZ is sensitive to surface effects when it is bound to or adsorbed onto membranes (Mateos-Gil et al. 2019 *FEMS Microbiol Rev* - DOI: 10.1093/femsre/fuy039). Therefore, the adsorption of FtsZ and ZapD onto the EM grid may influence the formation of higher order structures. In this study, we used cryo-electron microscopy (cryo-EM) and cryo-electron tomography (cryo-ET) to visualize the 3D organization of ZapD-mediated structures. This approach allows us to avoid staining artifacts and the distortion of structures caused by adsorption or drying of the grid. In addition, we can resolve single filaments. Our buffer conditions also differ slightly from those in previous studies, which may significantly impact the behavior of FtsZ, as illustrated in Supplementary Fig. 3.

> *At parts of the manuscript, the authors try a bit too hard to argue for the physiological significance of these toroids. This, however, is at least very questionable, because: The typical diameter is in the range of 0.25-1.0 µm, which requires some flexibility of the filaments to be able to accommodate this. It's difficult to see how a FtsZ-ZapD toroid, which appears to be quite rigid with a narrow size distribution of 502 nm {plus minus} 55 nm could support cell division rather than stalling it at that cell diameter. which the authors say is similar to the E. coli cell.*

The toroidal structures formed by FtsZ and ZapD, with their characteristics similar to those of the bacterial division system, are significant in physiological contexts and warrant further study. The connections mediated by Zaps are expected to play a crucial role in filament organization, which is vital for the machinery enabling cellular constriction. Therefore, characterizing these structures in vitro can provide insight into divisome stabilization, assembly and constriction mechanisms. While we acknowledge the limitations of in vitro systems and do not expect to see the same toroidal structures in vivo, the way ZapD decorates and connects FtsZ filaments *in vitro* may resemble the processes that occur in the division ring formed inside the cell. This study represents an initial effort to characterize these toroidal structures, which could inspire further research and potentially reveal their physiological relevance.

Regarding flexibility, it has been previously reported that an arrangement of loosely connected filaments forms the FtsZ ring. Our model is consistent with this observation despite the heterogeneity and density observed in the toroidal structures. We anticipate differences in vivo due to the high complexity of the cytoplasm, interactions with other cellular components, and attachment to the cell membrane, all of which would influence structural outcomes. However, our novel in vitro approach, which allows us to study FtsZ filament organization and connectivity – features that are challenging to explore in vivo and have not been thoroughly investigated before – has the potential to significantly advance our understanding of these structures. Consequently, these structures can aid our understanding of complex macrostructures in vivo, even if we have merely begun to scratch the surface of their characterization.

Regarding the size of the toroids, we hypothesize that it reflects an optimal condition based on our experimental setup in solution. *In vivo*, these conditions are altered by interactions with various division partners, attachment to the plasma membrane, and system contraction.

We have better reformulated and edited the manuscript to discuss the potential physiological relevance of our toroidal structures.

> *For cell division, FtsZ filaments are recruited to the membrane surface via an interaction of FtsA or ZipA the C-terminal peptide of FtsZ. As ZapD also binds to this peptide, the question arises who wins this competition or where is ZapD when FtsZ is recruited to the membrane surface? Can such a toroidal structure of FtsZ filaments form on the membrane surface? Additional experiments would be helpful, but a more detailed discussion on how the authors think ZapD could act on membrane-bound filaments would be essential.*

We appreciate this comment, which was indeed one of our main questions. The complexity of the division system raises many questions about the interaction of FtsZ with the plasma membrane. The competition between division components to interact with FtsZ and thus modulate its behavior is still largely unknown. FtsA and ZipA appear to have a greater affinity for the C-terminal domain (CTD) of FtsZ than ZapD. However, considering all FtsZ monomers forming a filament, we expect FtsZ filaments to interact with many different division partners. The ability of FtsZ to interact with many components is necessary to explain the current model of the system. According to this model, FtsZ filaments would be decorated by many different proteins, anchoring them to the membrane while crosslinking or promoting their disassembly in a spatiotemporally controlled manner.

We tried experiments combining FtsA, ZipA, and ZapD on supported lipid membranes and liposomes. However, they proved difficult to perform. We expect similar results to those observed for ZapA (Caldas et al. 2019 *Nat Commun* - DOI: 10.1038/s41467-019-13702-4). However, competition between proteins for interaction with the CTD of FtsZ adds an extra layer of complexity, making exploring this issue attractive in the future. However, as remarkably pointed out by Reviewer 3, our cryo-ET data of straight bundles provide new insights into how ZapD-FtsZ structures can bind to the plasma membrane. In these straight bundles, the CTDs of two parallel FtsZ filaments are oriented upwards. They can bind the plasma membrane directly or the ZapDs, which decorate the FtsZ filaments from above instead of from the side, as suggested previously (Schumacher et al. 2017 J Biol Chem - DOI: 10.1074/jbc.M116.773192), allowing ZapDs to interact with the membrane.

> *The authors conclude that the FtsZ filaments are dynamic, which is essential for cell division. But the evidence for dynamic FtsZ filaments within these toroids seems rather weak, as it is solely the partial reassembly after addition of GTP. As ZapD significantly slows down GTP hydrolysis, I am not sure it's obvious to make this conclusion.*

FtsZ filaments are dynamic, as they can reassemble into macrostructures relatively quickly. Decreased GTPase activity is a good indicator of the formation of lateral interactions between filaments. For instance, under crowding conditions, FtsZ also reduces its GTPase activity, although the bundles disassemble very slowly over time (González et al. 2003 J. Biol. Chem - DOI: 10.1074/jbc.M305230200). We measured the GTPase activity during the first 5 minutes after GTP addition, conditions under which toroidal structures and bundles remain fully assembled. However, we expect GTPase activity to recover as the macrostructures disassemble, considering the reassembly of macrostructures after GTP resupply, which suggests that FtsZ filaments remain active and dynamic.

> *On a similar note, on page 5 the authors claim that ZapD would transiently interact with FtsZ filaments. What is the evidence for this? They also say that this transient interaction could have a "mechanistic role in the functionality of FtsZ macrostructures." Could they elaborate?*

We have rephrased the whole paragraph in the revised version to clarify matters (page 10, lines 2434):

“These results are consistent with the observation that ZapD interacts with FtsZ through its central hub, which provides additional spatial freedom to connect other filaments in different conformations. This flexibility allows different filament organizations and contributes to structural heterogeneity. In addition, these results suggest that these crosslinkers can act as modulators of the dynamics of the ring structure, spacing filaments apart and allowing them to slide in an organized manner. The ability of FtsZ to treadmill directionally, together with the parallel or antiparallel arrangement of short, transiently crosslinked filaments, is considered essential for the functionality of the Z ring and its ability to exert constrictive force34,36–38,50. Thus, Zap proteins can play a critical role in ensuring correct filament placement and stabilization, which is consistent with the toroidal structure formed by ZapD.”

> *The author should also improve in putting their findings into the context of existing knowledge. For example:*

The authors observe a straightening of filament bundles with increasing ZapD concentration. This seems consistent with what was found for ZapA, but this is not explicitly discussed (Caldas et al 2019)

We have discussed this similarity in the revised version of this manuscript (page 12, line 40 - page 13, line 8):

“Understanding how the associative states of ZapA (as tetramers) and ZapD (as dimers), together with membrane tethering, influence the predominant structures formed in both systems is essential. The complexity of the division system raises important questions about the interaction dynamics between FtsZ and the plasma membrane. The competitive nature of the division components to engage with FtsZ and modulate its functionality remains to be thoroughly elucidated. It is important to note that FtsA and ZipA have a greater affinity for the C-terminal domain of FtsZ than ZapD. Our cryo-ET data on straight bundles provide new perspectives on how ZapD-FtsZ structures can effectively bind to the plasma membrane; in particular, the C-terminal domains of parallel FtsZ filaments are oriented upward, allowing direct membrane binding or interaction with ZapDs that reinforce these filaments from above, rather than from the side, as previously suggested.”

> *A paragraph summarizing what is known about the properties of ZapD in vivo would be essential: i.e., what has been found regarding its intracellular copy number, location and dynamics?*

We thank the reviewer for this valuable suggestion. We describe the role of Zap proteins in vivo and the previous studies of ZapD in the introduction (page 2, lines 34 - page 3, line 17). Additionally, we added the estimated number of ZapD copies in the cell in the discussion (page 11, lines 2-7).

> *In the introduction, the authors write that "GTP binding and hydrolysis induce a conformational change in each monomer that modifies its binding potential, enabling them to follow a treadmilling behavior". This seems inaccurate, as shown by Wagstaff et al. 2022, the conformational change of FtsZ is not associated with the nucleotide state. In addition, they write that FtsZ polymerization depends on the GTPase activity. It would be more accurate to write that polymerization depends on GTP, and disassembly on GTPase activity.”*

Following the reviewer's suggestions, we have adapted and corrected these text elements as follows (page 2, lines 7-9):

“FtsZ undergoes treadmilling due to polymerization-dependent GTP hydrolysis, allowing the ring to exhibit its dynamic behavior.”

> *On page 2 they also write that "the mechanism underlying bundling of FtsZ filaments is unknown". I would disagree, the underlying mechanism is very well known (see for example Schumacher, MA JBC 2017), but how this relates to the large-scale organization of FtsZ filaments was not clear.*

We thank the reviewer for this comment. We have corrected and clarified the related text accordingly (page 3, lines 11-12):

“…the link between FtsZ bundling, promoted by ZapD, and the large-scale organization of FtsZ filaments remains unresolved.”

> *The authors describe the toroid as a dense 3D mesh, how would this be compatible with the Z-ring and its role for cell division? I don't think this corresponds to the current model of the Z-ring (McQuillen & Xiao, 2020). Apart from the fact it's a ring, I don't think the organization of FtsZ obviously similar to the current of the Z-ring in the bacterial cell, in particular because it's not obvious how FtsZ filaments can bind ZapD and membrane anchors simultaneously.*

We consider that the intrinsic characteristics of toroidal structures and the bacterial division ring have points in common. As indicated in the answer above, despite the differences and limitations that might result from an in vitro approach, the structures shown after ZapD crosslinking of FtsZ filaments can demonstrate intrinsic features occurring in vivo. The current model of the division ring consists of an arrangement of filaments loosely connected by crosslinkers in the center of the cell, forming a ring. This model is compatible with our findings, although many questions remain about the structural organization of the Z-ring in the cell.

Reviewer 3 has brought a compelling new perspective to interpreting our cryo-ET data: ZapD decorates FtsZ from above, allowing ZapD or FtsZ to bind to the plasma membrane. We have discussed this point in more detail below. In the case of straight bundles, this favors the stacking of straight FtsZ filaments, whereas in the case of toroids, ZapD can also bind FtsZ filaments laterally and diagonally, and it is this less compact arrangement that could enable FtsZ bending and toroid size adjustment.

We have revised the text accordingly to incorporate the interpretation proposed by Reviewer 3 (page 12, lines 24-31):

“The current model of the division ring consists of an array of filaments loosely connected by crosslinkers at the center of the cell, forming a ring. This model is consistent with our findings, although many questions remain regarding the structural organization of the Z ring within the cell. ZapD binds to FtsZ from above, allowing either ZapD or FtsZ to interact with the plasma membrane. In straight bundles, this facilitates the stacking of straight FtsZ filaments, while for toroids, ZapD can also bind FtsZ filaments diagonally. This less compact arrangement could allow bending of the FtsZ filaments and adjustment of toroid size.”

> *The authors write that "most of these modulators" interact with FtsZ's CTP, but then later that ZapD is the only Zap protein that binds CTP. This seems to be inconsistent. Why not write that membrane anchors usually bind the CTP, most Zaps do not, but ZapD is the exception?*

We thank the reviewer for this pertinent suggestion, which we have followed in the revised version of the manuscript (page 2, lines 19-22):

"Most of these modulators interact with FtsZ through its carboxy-terminal end, which modulates division assembly as a central hub. ZapD is the only Zap protein known to crosslink FtsZ by binding its C-terminal domain, suggesting a critical Z ring structure stabilizing function."

> *I also have some comments regarding the experiments and their analysis:*
>
> *Regarding cryoET: the filaments appear like flat bands, even in the absence of ZapD, which further elongates these bands. Is this due to an anisotropic resolution? This distortion makes the conclusion that ZapD forms bi-spherical dimers unconvincing.*

The missing wedge caused by the limited angular range of the tomography data generates an elongation of the structures by a factor of 2 along the Z axis. This feature is visible in the undecorated FtsZ filament data (Supplementary Fig. 10). The more pronounced elongation along the Z-axis observed in the presence of ZapD indicates the presence of ZapD to connect two parallel FtsZ filaments along the Z-axis (see Supplementary Figs. 8, 9 and 10). We do not have sufficient resolution to precisely resolve ZapD proteins from the FtsZ filaments in the Z-axis, but we also observed bispherical ZapDs in the XY plane (Fig. 4b-d). Unfortunately, our data do not allow for a more detailed characterization.

> *The authors say that the cryoET visualization provides crucial information on the length of the filaments within this toroid. How long are they? Could the authors measure it?*

Measuring the length of single filaments is not trivial, given the dense, heterogeneous mesh promoted by ZapD crosslinking. We tried to identify and track them, but the density of filaments and connections made precise measurement very difficult. Nevertheless, we could identify the formation of these toroids by an arrangement of short filaments (Supplementary Fig. 11) instead of continuous circular filaments.

We have removed the following sentence text in the revised manuscript: "Visualization of ZapDmediated FtsZ toroidal structures by cryo-ET provided crucial information on the 3D organization, connectivity and length of filaments within the toroid."

> *Regarding the dimerization mutant of ZapD: there is actually no direct confirmation that mZapD is monomeric. Did the authors try SEC MALS or AUC? Accordingly, the statement that dimerization is "essential" seems exaggerated (although likely true).*

Unlike the wild-type ZapD protein, the mZapD mutant exists as a mixture of monomers (~15%) and dimers, as AUC assays performed at similar protein concentrations revealed. These results demonstrate that the mutant protein has a lower tendency to form dimers than the native ZapD protein. We have included the AUC data for mZapD in the supplementary material (Supp. Fig. 15a).

> *What do the authors mean that toroid formation is compatible with robust persistence length? I.e. What does robust mean? It was recently shown that FtsZ filaments are actually surprisingly flexible, which matches well the fact that the diameter of the Z-ring must continuously decrease during cell division (Dunajova et al Nature Physics 2023).*

We have corrected this sentence in the revised version of the manuscript to improve clarity (page 11, lines 9-10):

"The persistence length and curvature of FtsZ filaments are optimized for forming bacterial-sized ring structures."

> *The authors claim that their observations suggest „that crosslinkers ... allows filament sliding in an organized fashion". As far as I know there is no evidence of filament sliding, as FtsZ monomers in living cells and in vitro are static.*

Filament sliding may be one of the factors contributing to the force generation mechanisms involved in cell division (Nguyen et al. 2021 J Bacteriol - DOI: 10.1128/JB.00576-20). Our results indicate that ZapD can separate filaments, creating space between them and facilitating their organization.

Although the molecular dynamics of cell constriction are not yet fully understood, it is possible that filament sliding plays a role. If this is the case, the crosslinking of short FtsZ filaments in multiple directions by ZapD could provide the necessary flexibility to adjust the diameter of the constriction ring during bacterial division.

> *What is the „proto-ring FtsA protein"?*

The proto-ring denotes the first molecular assembly of the Z-ring, which in E. coli consists of FtsZ, FtsA and ZipA (see, for example, Ortiz et al. 2016 FEMS Microbiol Rev - DOI: 10.1093/femsre/fuv040). To simplify matters, we have deleted the term “proto-ring” in the revised version of the MS.

> *The authors refer to „increasing evidence" for „alternative network remodeling mechanisms that do not rely on chemical energy consumption as those in which entropic forces act through diffusible crosslinkers, similar to ZapD and FtsZ polymers." A reference should be given, I assume the authors refer to the study by Lansky et al 2015 of PRC on microtubules. However, I am not sure how the authors made the conclusion that this applies to FtsZ and ZapD, on which evidence is this assumption based?*

We refer to cytoskeletal network remodeling mechanisms independent of chemical energy consumption (Braun et al. 2016 *Bioessays* - DOI: 10.1002/bies.201500183) driven by entropic forces induced by macromolecular crowding agents or diffusible crosslinkers. The latter mechanism leads to an increase in filament overlap length and the contraction of filament networks. These mechanisms complement and act in synergy with energy-consuming processes (such as those involving nucleotide hydrolysis) to modulate actin- and microtubule-based cytoskeleton remodeling. Similarly, crosslinking proteins such as ZapD may contribute to remodeling the FtsZ division ring in the cell.

We have revised the corresponding text of the manuscript accordingly (page 13, lines 16-24): “In addition, our findings could greatly enhance the understanding of how polymeric cytoskeletal networks are remodeled during essential cellular processes such as cell motility and morphogenesis. Although conventional wisdom points to molecular motors as the primary drivers of filament remodeling through energy consumption, there is increasing evidence that there are alternative mechanisms that do not rely on such energy, instead harnessing entropic forces via diffusible crosslinkers. This approach may also be applicable to ZapD and FtsZ polymers, suggesting a promising avenue for optimizing conditions in the reverse engineering of the division ring to enhance force generation in minimally reconstituted systems aimed at achieving autonomous cell division.”

> *Some inconsistencies in supplementary figure 3: The normalized absorbances in panel a do not seem to agree with the absolute absorbance shown in panel e, i.e. compare maximum intensity for ZapD = 20 μM and 5 μM in both panels.*

We have corrected these inconsistencies in the revised version.

> *It's not obvious to me why the structure formed by ZapD and FtsZ disassembles after some time even before GTP is exhausted, can the authors explain? As the structures disassemble, how is the "steadystate turbidity" defined? Do the structures also disassemble when they use a non-hydrolyzable analog of GTP?*

In the presence of ZapD, FtsZ rapidly forms higher order polymers after the addition of GTP, as shown by turbidity assays at 320 nm (the formation of single- or double-stranded FtsZ filaments in the absence of ZapD does not produce a significant increase in turbidity). Macrostructures formed by FtsZ in the presence of ZapD, while more stable than FtsZ filaments (which rapidly disassemble following GTP consumption), are also dynamic. These assembly reactions are GTP-dependent and considerably modify polymer dynamics. In agreement with our results, previous studies have shown that high concentrations of macromolecular crowders (such as Ficoll or dextran) promote the formation of dynamic FtsZ polymer networks (González et al. 2003 J. Biol. Chem - DOI: 10.1074/jbc.M305230200). In this case, FtsZ GTPase activity was significantly retarded compared with FtsZ filaments, resulting in a decrease in GTPase turnover. Similar mechanisms may apply to assembly reactions in the presence of ZapD.

Parallel assembly studies replacing GTP with a slowly hydrolyzable GTP analog remain pending. We expect ZapD-containing FtsZ macrostructures to last assembled for longer but still disassemble upon GTP consumption, as occurs with the crowding-induced FtsZ polymer networks formed in the presence of nucleotide analogs.

Accordingly, we have revised the corresponding text to clarify matters (page 4, line 37 – page 5 line 7).

> *Conclusion: Despite some weaknesses in the interpretation of their findings, I think this paper will likely motivate other structural studies on large scale assemblies of FtsZ filaments and its associated proteins. A systematic comparison of the effects of ZapA, ZapC and ZapD and how their different modes of filament crosslinking can result in different filament networks will be very useful to understand their individual roles and possible synergistic behavior.*

We appreciate the reviewer's remarks and comments, which provided us with valuable information and helped us considerably improve the revised manuscript.

> ***Reviewer #3 (Public Review):***
>
> *Summary:*
>
> *The authors provide the first image analysis by cryoET of toroids assembled by FtsZ crosslinked by ZapD. Previously toroids of FtsZ alone have been imaged only in projection by negative stain EM. The authors attempt to distinguish ZapD crosslinks from the underlying FtsZ filaments. I did not find this distinction convincing, especially because it seems inconsistent with the 1:1 stoichiometry demonstrated by pelleting. I was intrigued by one image showing straight filament pairs, which may suggest a new model for how ZapD crosslinks FtsZ filaments.*

We thank the reviewer for these valuable comments, to which we have responded in detail below.

> *Strengths:*
>
> *(1) The first image analysis of FtsZ toroids by cryoET.*

> *(2) The images are accompanied by pelleting assays that convincingly establish a 1:1 stoichiometry of FtsZ:ZapD subunits.*
>
> *(3) Fig. 5 shows an image of a pair of FtsZ filaments crosslinked by ZapD. This seems to have higher resolution than the toroids. Importantly, it suggests a new model for the structure of FtsZ-ZapD that resolves previously unrecognized conflicts. (This is discussed below under weaknesses, because it is so far only supported by a single image.)*

We thank the reviewer for this assessment and, in particular, for raising point 3, which provided a new perspective on the interpretation of our data. We have also included a new example of a straight bundle in Supplementary Fig. 13.

> *Weaknesses:*
>
> *This paper reports a study by cryoEM of polymers and bundles assembled from FtsZ plus ZapD. Although previous studies by other labs have focused on straight bundles of filaments, the present study found toroids mixed with these straight bundles, and they focused most of their study on the toroids. In the toroids they attempt to delineate FtsZ filaments and ZapD crosslinks. A major problem here is with the stoichiometry. Their pelleting assays convincingly established a stoichiometry of 1:1, while the mass densities identified as ZapD are sparse and apparently well below the number of FtsZ (FtsZ subunits are not resolved in the reconstructions, but the continuous sheets or belts seem to have a lot more mass than the identified crosslinks.)*
>
> *Apart from the stoichiometry I don't find the identification of crosslinks to be convincing. It is missing an important control - cryoET of toroids assembled from pure FtsZ, without ZapD.*
>
> *However, if I ignore these and jump to Fig. 5, I think there is an important discovery that resolves controversies in the present study as well as previous ones, controversies that were not even recognized. The controversy is illustrated by the Schumacher 2017 model (their Fig. 7), which is repeated in a simplified version in Fig. 1a of the present mss. That model has a two FtsZ filaments in a plane facing ZapD dimers which bridge them. In this planar model the C-terminal linker, and the ctd of FtsZ that binds ZapD facing each other and the ZapD in the middle, with. The contradiction arises because the C-terminus needs to face the membrane in order to attach and generate a bending force. The two FtsZ filaments in the planar model are facing 90{degree sign} away from the membrane. A related contradiction is that Houseman et al 2016 showed that curved FtsZ filaments have the C terminus on the outside of the curve. In a toroid the C termini should all be facing the outside. If the paired filaments had the C termini facing each other, they could not form a toroid because the two FtsZ filaments would be bending in opposite directions.*
>
> *Fig. 5 of the present ms seems to resolve this by showing that the two FtsZ filaments and ZapD are not planar, but stacked. The two FtsZ filaments have their C termini facing the same direction, let's say up, toward the membrane, and ZapD binds on top, bridging the two. The spacing of the ctd binding sites on the Zap D dimer is 6.5 nm, which would fit the ~8 nm width of the paired filament complex observed in the present cryoEM (Fig S13). In the Schumacher model the width would be about 20 nm. Importantly, the stack model has the ctd of each filament facing the same direction, so the paired filaments could attach to the membrane and bend together (using ctd's not bound by ZapD). Finally, the new arrangement would also provide an easy way for the complex to extend from a pair of filaments to a sheet of three or four or more. A problem with this new model from Fig. 5 is that it is supported by only a single example of the paired FtsZ-ZapD complex. If this*

> *is to be the basis of the interpretation, more examples should be shown. Maybe examples could be found with three or four FtsZ filaments in a sheet.*

We thank the reviewer for asking interesting questions and suggesting a compelling model for how ZapD could bind FtsZ filaments. Cryo-ET of straight bundles revealed that high ZapD density promotes vertical stacking of FtsZ filaments and decoration of FtsZ filaments by ZapD from above. In toroids, FtsZ filaments are vertically decorated by ZapD, which explains the high elongation of the filament structures observed, consisting of FtsZ-ZapD(-FtsZ) units. In addition, we observed a high abundance of diagonal connections between FtsZ filaments of different heights, revealing a certain flexibility/malleability of ZapD to link filaments that are not perfectly aligned vertically. This configuration could give rise to curved filaments and the overall toroid structure.

The manuscript proposes that ZapD can bind FtsZ filaments in different directions. However, it seems to have a certain tendency to bind to the upper part of FtsZ filaments, stacking them vertically or vertically with a lateral shift (Supplementary Fig. 9). We also observe lateral connections, although the features of the toroidal structures limit their visualization. This enables both the binding to the membrane by ZapD or FtsZ and the formation of higher order FtsZ polymer structures.

In summary, ZapD is capable of linking FtsZ filaments in multiple directions, including from the upper part of the filaments as well as laterally or diagonally. At high concentrations of ZapD, the filaments become more compactly arranged, primarily stacking vertically, which results in the loss of curvature. In contrast, at lower concentrations of ZapD, the FtsZ filaments are less tightly packed, leading to curved filaments and an overall toroidal structure that may resemble the in vivo ring structures.

We have edited our manuscript to accommodate this hypothesis, including the abstract and the cryoET section (page 7, lines 5-16):

“The isosurface confirmed the presence of extended structures along the Z-axis, well beyond the elongation expected from the missing wedge effect for single FtsZ filaments (for comparison, see Supplementary Fig. 10). The vertically extended structures appeared to correspond to filaments that were connected or decorated by additional densities along the Z-axis (Supplementary Fig. 9b). Importantly, these densities were only observed in the presence of ZapD (Supplementary Fig. 10b), suggesting that they represent ZapD connections (Fig. 3e and Supplementary Figs. 8e and 9b). We note that the resolution of the data is not sufficient to precisely resolve ZapD proteins from the FtsZ filaments in the Z-axis.

These results suggest that the toroids are constructed and stabilized by interactions between ZapD and FtsZ, which are mainly formed along the Z-axis but also laterally and diagonally.”

Page 7, lines 40-42:

“Cryo-ET imaging of ZapD-mediated FtsZ toroidal structures revealed a preferential vertical stacking and crosslinking of short ZapD filaments, which are also crosslinked laterally and diagonally, allowing for filament curvature.”

And in the discussion (page 12, lines 27-31):

“ZapD binds to FtsZ from above, allowing either ZapD or FtsZ to interact with the plasma membrane. In straight bundles, this facilitates the stacking of straight FtsZ filaments, while for toroids, ZapD can also bind FtsZ filaments diagonally. This less compact arrangement could allow bending of the FtsZ filaments and adjustment of the toroid size.”

> *What then should be done with the toroids? I am not convinced by the identification of ZapD as "connectors." I think it is likely that the ZapD is part of the belts that I discuss*

> *below, although the relative location of ZapD in the belts is not resolved. It is likely that the resolution in the toroid reconstructions of Fig. 4, S8,9 is less than that of the isolated pf pair in Fig. 5c.*

We agree with the reviewer's interpretation that ZapD can attach to FtsZ filaments from both above and laterally. The data from the straight bundles, which are more clearly resolved due to their thinner structure, demonstrate that ZapD can decorate FtsZ filaments vertically. Additionally, the toroidal data supports the notion that ZapD can act as a crosslinker between filaments that are not perfectly vertical, allowing for lateral offsets (see, for example, Fig. 4d) or lateral connections (Fig. 4b).

We recognize that the resolution and high density of structures in our cryo-ET data make it challenging to accurately annotate proteins or connectors. Despite this difficulty, we have made efforts to label and identify the ZapD proteins and connectors. We employed an arbitrary labeling method to assist with visual interpretation. However, we acknowledge that some errors may exist and that ZapD proteins were not labeled, particularly along the Z-axis, where the missing wedge limits our ability to distinguish between ZapD and FtsZ proteins (page 7, lines 8-13):

“The vertically extended structures appeared to correspond to filaments that were connected or decorated by additional densities along the Z-axis (Supplementary Fig. 9b). Importantly, these densities were only observed in the presence of ZapD (Supplementary Fig. 10b), suggesting that they represent ZapD connections (Fig. 3e and Supplementary Figs. 8e and 9b). We note that the resolution of the data is not sufficient to precisely resolve ZapD proteins from the FtsZ filaments in the Z-axis. We note that the resolution of the data is not sufficient to precisely resolve ZapD proteins from the FtsZ filaments in the Z-axis.”

We draw attention to the limitation of our manual segmentation in the text as follows (page 7, lines 20-24):

“We manually labeled the connecting densities in the toroid isosurfaces to analyze their arrangement and connectivity with the FtsZ filaments. The high density of the toroids and the wide variety of conformations of these densities prevented the use of subtomogram averaging to resolve their structure and spatial arrangement within the toroids.”

> *Importantly, If the authors want to pursue the location of ZapD in toroids, I suggest they need to compare their ZapD-containing toroids with toroids lacking ZapD. Popp et al 2009 have determined a variety of solution conditions that favor the assembly of toroids by FtsZ with no added protein crosslinker. It would be very interesting to investigate the structure of these toroids by the present cryoEM methods, and compare them to the FtsZ-ZapD toroids. I suspect that the belts seen in the ZapD toroids will not be found in the pure FtsZ toroids, confirming that their structure is generated by ZapD.*

The only reported toroidal structure of E. coli FtsZ can be found in the literature by Popp et al. (2009 Biopolymers – DOI: 10.1002/bip.21136). It is important to note that methylcellulose (MC) must be added to the working solution to induce the formation of these structures, as FtsZ toroids do not form in the absence of MC. The mechanisms by which MC promotes this assembly process go beyond mere excluded volume effects due to crowding, as the concentration of MC used is very low (less than 1 mg/ml), which is below the typical crowding regime. This suggests that there are additional interactions between MC and FtsZ. Such complexities and secondary interactions prevent the use of this system as a reliable control for the FtsZ toroidal structures reported here. Alternatively, we also considered the toroidal structures of FtsZ from Bacillus subtilis (Huecas et al. 2017 Biophys J - DOI: 10.1016/j.bpj.2017.08.046) and Cyanobacterium synechocystis (Wang et al. 2019 J Biol Chem –

DOI: 10.1074/jbc.RA118.005200). However, these structures do not serve as appropriate controls due to the structural and molecular differences between these FtsZ proteins.

> ***Recommendations for the authors:***
>
> ***Reviewing Editor:***
>
> *While the three referees recognize and appreciate the importance of this work several technical and interpretational questions have been raised. There was a prolonged discussion amongst the three expert referees, and it was felt that the current version suffers from a number of problems that the authors need to consider. These are to do with 1. Stoichiometry of ZapD-FtsZ 2. the evidence for crosslinks 3. how the cryo-ET data correlates with the biophysical data 4. Physiological relevance of the elucidated structures. Please take note of the public reviews (strengths and weaknesses) as well as "Recommendations to the authors" sections below, if you choose to prepare a revision.*
>
> *In reading the reviews very carefully (as well as while following the ensuing robust discussion between the referees) I noticed that all points raised are extremely important to be addressed / reconciled (with experiments and / or discussion) for this study to become an outstanding contribution to bacterial cell biology field. I would therefore urge you to consider these carefully and revise the manuscript accordingly.*

We thank the editorial board and reviewers for their excellent work evaluating and reviewing our manuscript. Their constructive suggestions and comments have been taken into account in preparing the revised version. We have paid particular attention to the four points mentioned above by the reviewing editor. We hope that the new version and this point-by-point rebuttal letter will answer most of the questions and weaknesses raised by the reviewers.

> ***Reviewer #1 (Recommendations for the authors):***
>
> *Suggestions for improvement of the manuscript:*
>
> *(1) ZapD to FtsZ ratio:*
>
> *i) Page 3: Results section, paragraph 1:*
>
> *FtsZ to ZapD shows a 1:2 ratio. How does this explain cross linking by a dimeric species, as this will be equivalent to a 1:1 ratio of FtsZ and ZapD? The crystal structure in the reference cited has FtsZ peptide bound only to one side of the dimer, however a crosslinking effect can happen only if FtsZ binds to both protomers of ZapD dimer. If the decoration is not uniform as given in the toroid model based on cryoET, this should lead to a model with excess of FtsZ in the toroid?*

On page 3 of the original manuscript, we stated that the binding stoichiometry of ZapD to FtsZ was 2:1, based on estimates derived from sedimentation velocity experiments involving the unassembled GDP form of FtsZ. However, upon reanalyzing these experiments, we found that the previous characterization of the association mode was overly simplistic. We determined that there are two predominant molecular species of ZapD:FtsZ complexes in solution, which correspond to ZapD dimers bound to either one or two FtsZ monomers, resulting in stoichiometries of 2:1 and 1:1, respectively. The revised binding stoichiometry data for ZapD and GDP-FtsZ suggests the presence of 1:1 ZapD-FtsZ complexes which aligns with the idea that FtsZ polymers can be crosslinked by dimeric ZapD species. In mixtures where ZapD is present in excess over FtsZ, the crosslinking corresponds to 1:1 binding stoichiometries, leading to the formation of straight macrostructures. Conversely, when the concentration of ZapD is reduced in the reaction mixture, the resulting macrostructures take the form of

toroids. In this scenario, there is an excess of FtsZ because only some of the FtsZ molecules within the polymers are crosslinked by ZapD dimers, resulting in a binding stoichiometry of approximately 0.4 ZapD molecules per FtsZ, as quantified by differential sedimentation experiments.

We have rewritten the corresponding texts in the revised version to explain these matters (page 4 lines 14-18):

“Sedimentation velocity analysis of mixtures of the two proteins revealed the presence of two predominant molecular species of ZapD:FtsZ complexes in solution. These complexes are compatible with ZapD dimers bound to one or two FtsZ monomers, corresponding to ZapD:FtsZ stoichiometries of 2:1 and 1:1, respectively (Supplementary Fig. 1a (III-IV)). This observation is consistent with the proposed interaction model.”

> *ii) How does 40 - 80 uM of ZapD correspond to a molar ratio of approximately 6?*

It was a typo from previous versions. We have corrected it in the revised version.

> *iii) The ratios of ZapD to FtsZ are different when described later in page 4 in the context of the toroid. Are these ratios relevant compared to the contradicting ratios mentioned later in page 4?*

To clarify issues related to the binding of ZapD to FtsZ, we have rewritten the sections on ZapD binding stoichiometries to both FtsZ-GDP and FtsZ polymers in the presence of GTP (see page 4 lines 14-18 and page 5 lines 15-26).

> *iv) Supplementary Figure 5:*
>
> *In the representative gel shown, the amount of ZapD in the pellet does not appear to be double compared to 10 and 30 uM concentrations. However, the estimated amount in the plot shown in panel (c) appears to indicate that that ZapD has approximately doubled at 30 uM compared to 10 uM. Please re-check the quantification.*

Without prior staining calibration of the gels, there is no simple quantitative relationship between gel band intensities after Coomassie staining and the amount of protein in a band (Darawshe et al. 1993 Anal Biochem - DOI: 10.1006/abio.1993.1581). The latter point precludes a quantitative comparison of pelleting / SDS-PAGE data and analytical sedimentation measurements.

> *v) How can a consistent ratio being maintained be explained in an irregular structure of the toroid? The number of ZapD should be much less compared to FtsZ according to the model.*

See answers to points i) and iii)

> *(2) GTPase activity and assembly/disassembly of toroids:*
>
> *i) Page 3, Results section: last paragraph:*
>
> *What is the explanation or hypothesis for decrease in GTPase activity upon ZapD binding? Given that FtsZ core is not involved in the interaction of the higher order assemblies, what is the probable reason on decrease in GTPase activity upon ZapA binding?*

Excluded volume effects caused by macromolecular crowding, such as high concentrations of Ficoll or dextran, promote the formation of dynamic FtsZ polymer networks (González et al.

2003 J. Biol. Chem - DOI: 10.1074/jbc.M305230200). In these conditions, FtsZ GTPase activity is significantly slowed down compared to the activity observed in FtsZ filaments formed without crowding, leading to a decreased GTPase turnover rate. Similar mechanisms may also apply to assembly reactions in the presence of ZapD (see, for example, Durand-Heredia et al. 2012 J Bacteriol - DOI: 10.1128/JB.0017612).

> *ii) How is the decrease in GTPase activity compatible with dynamics of disassembly? Please substantiate on why disassembly is linked to transient interaction with ZapD. Shouldn't disassembly and transient interaction be linked to recovery of GTPase activity rates?*
>
> *iii) Does the decrease in GTPase activity imply a reduced turnover of disassembly of FtsZ to monomers? Hence, how is the reduction in turbidity related to the decrease in GTPase activity? How does the GTPase activity change with time? iv) How can the decrease in GTPase activity with increasing ZapD be explained?*

We conducted GTPase activity assays within the first two minutes following GTP addition, a timeframe that promotes bundle formation. Previous studies, such as those by Durand-Heredia et al. (2012 *J Bacteriol* - DOI: 10.1128/JB.00176-12), have also indicated a reduction in GTPase activity during the initial moments of bundling. The reviewer's suggestion that GTPase activity should recover after the disassembly of toroids is valid and warrants further investigation. To test this hypothesis, measuring GTPase activity over extended periods would be necessary. When comparing FtsZ filaments observed in vitro, we found that ZapD-containing FtsZ bundles exhibit decreased GTPase activity. Although we did not measure it directly, we anticipate a reduction in the rate of GTP exchange within the polymer, similar to the behavior of FtsZ bundles formed in the presence of crowders (González et al. 2003 *J. Biol. Chem* - DOI: 10.1074/jbc.M305230200), which also display a delay in GTPase activity. High levels of ZapD enhance bundling, which may explain the decrease in GTPase activity as ZapD levels increase.

> *(3) Treadmilling and FtsZ filament organisation:*
>
> *If the FtsZ filaments are cross linked antiparallel, how can tread milling behaviour be explained? Doesn't tread milling imply a directionality of filament orientations in the FtsZ bundles?*

Our model can only suggest filament alignment. The latter is compatible with parallel and antiparallel filament organization.

> *The correlation between observed effects on GTPase activity, treadmilling and ZapD interaction will provide an interesting insight to the model.*

Establishing a detailed correlation among these three factors could yield valuable insights into the mechanisms and potential physiological implications of the structural organization of FtsZ polymers influenced by crosslinking proteins and ZapD. To precisely characterize these interactions, further time-resolved assays in solution and reconstituted systems would be necessary, which is beyond the scope of this study.

> *(4) Toroid dimensions and intrinsic curvature:*
>
> *i) Page 4: What is the correlation between the toroid dimensions and the intrinsic curvature of the FtsZ filaments? Given the thickness of ~ 127 nm, please provide an explanation of how the intrinsic curvature of FtsZ is compatible with both the inner and outer diameters of 500 nm and 380 nm.*

We added a paragraph for clarification (page 6, lines 20-24):

“Previous studies have shown different FtsZ structures at different concentrations and buffer conditions. FtsZ filaments are flexible and can generate different curvatures ranging from mini rings of ~24 nm to intermediate circular filaments of ~300 nm or toroids of ~500 nm in diameter (reviewed in Erickson and Osawa 2017 Subcell Biochem - DOI: 10.1007/978-3-319-53047-5_5, and Wang et al. 2019 J Biol Chem - DOI: 10.1074/jbc.RA119.009621). It is reasonable to assume that FtsZ filaments can accommodate the toroid shape promoted by ZapD crosslinking.”

> *ii) For the curvature of FtsZ filaments to be similar, the length of the filaments in the inner circles of the toroid have to be smaller than those in the outer circles? Is this true? Or are the FtsZ filaments of uniform length throughout?*

Due to the limitations in the resolution of the toroidal structure, we could not accurately measure the length or curvature of the filaments. Considering the FtsZ flexibility, these filaments may exhibit various curvatures and lengths, as previously mentioned.

> *iii) Is the ZapD density uniform thought the inner and outer regions of the toroid?*

The heterogeneity found in the structures suggests a difference in ZapD binding densities; however, we lack quantitative data to confirm this. The outer regions are likely more exposed to the attachment of free ZapDs in the surrounding environment, which leads to the recruitment of more ZapDs and the formation of straight bundles. Supplementary Fig. 7b (right) features a zoomed-in image of a toroid adorned with globular densities in the outer areas, which may correspond to ZapD oligomers. Similar characteristics appear in the straight filaments illustrated in the panels of this figure. However, these features are absent or present in significantly lower quantities in toroids with a 1:1 ratio and toroids formed under a 1:6 ratio, suggesting that the external decoration is due to ZapD saturation. Unfortunately, we cannot provide further details on the characteristics of these protein associations.

> *(5) Regular arrangement and toroid structure:*
>
> *i) Page 4: last section, first sentence: What is meant by 'regular' arrangement here? The word regular will imply a periodicity, which is not a feature of the bundles.*

We have rephrased the sentence in the revised manuscript as follows (page 5, lines 35-36): “Previous studies have visualized bundles with similar features using negative-stain transmission electron microscopy.”

> *ii) Similarly, page 6 first sentence mentions about a conserved toroid structure. Which aspects of the toroid structure are conserved and what are the other toroids that are compared with?*

We noted several features that are conserved in the ZapD-mediated toroidal structures, including their diameter, thickness, height, and roundness, as shown in Fig. 2d-e and Supplementary Fig. 6b-c. However, the internal organization of the toroid does not exhibit a periodic or regular structure. We have rephrased this to say: “…resulting in a toroidal structure observed for the first time following the interaction between FtsZ and one of its natural partners in vitro.” (page 7, lines 42-43):

> *iii) Discussion, para 1, last sentence: How is the toroid structural correlated with the bacterial cell FtsZ ring? What do the authors mean by 'structural compatibility' with the*

> *ring?*

The toroidal structures described in this work are consistent with the intermediate curved conformation of FtsZ polymers observed more generally across bacterial species and are likely to be part of the FtsZ structure responsible for constriction-force generation (Erickson and Osawa 2017 Subcell Biochem - DOI: 10.1007/978-3-319-53047-5_5). In the case of *E. coli*, if we assume an average of around 5000 FtsZ monomers in the polymeric form (two-thirds of the total found in dividing cells), this number of FtsZ molecules would be enough to encircle the cell around 6-8 times (considering the axial spacing between FtsZ monomers and the cell perimeter), which would be compatible with the structure adopting the form of a discontinuous toroidal assembly.

The term “structural compatibility” could be confusing, so we have removed it from the revised text.

> *iv) Discussion, para 2:*
>
> *Resemblance with the division ring in bacterial cells is mentioned in paragraph 2, however the features that are compared to claim resemblance comes later in the discussion. It will be helpful to rearrange the sections so that these are presented together.*

We have reorganized the sections following the reviewer’s suggestion.

> *(6) CryoET of toroid and interpretation of the tomogram:*
>
> *i) Supplementary figure 10: It is not convincing that the indicated densities correspond to ZapD. Is the resolution and the quality of the tomogram sufficient to comment on the localisation of ZapD? It is challenging to see any interpretable difference between FtsZ filament dimers in 10a vs FtsZ+ZapD in panel (b).*

We acknowledge that localizing ZapDs in the structure is a challenge due to the limited resolution of the cryo-ET data (page 7, lines 11-13, 21-24). We have manually labeled putative ZapDs in the data and have done our best to identify the structures reasonably while recognizing the limitations of the segmentation. We use different colors to guide the eye without clearly stating what is or is not a ZapD. However, filaments found in 1:1 and 1:6 ratio toroids have a clear difference in thickness to those observed in the absence of ZapD. The filaments in 1:0 ratio toroids provide a reasonable control for elongation due to the missing wedge and allow us to attribute the extra filament thickness to ZapD densities confidently (page 7, lines 5-12).

> *ii) How is it quantified that the elongation in Z is beyond the missing wedge effect? Please include the explanation for this in the methods or the relevant data as Supplementary figure panels.*

The missing wedge effect causes an elongation by a factor of 2 along the Z-axis. This elongation is evident in the filaments of the 1:0 ratio toroids. Consequently, the elongation in the filaments of the 1:1 and 1:6 ratio toroids exceed that observed due to the missing wedge effect. We have also added this information to the methods section (page 17, lines 31-33).

> *iii) Segmentation analysis of the tomogram and many method details of analysis and interpretation of the tomography data has not been described. This is essential to understand the reliability of the interpretation of the tomography data.*

We provided thresholds for volume extraction as isosurfaces and clarified how the putative ZapDs are colored in the revised methods section (page 17, line 24-30). However, we could not perform quantitative analysis of the segmented structures.

> *(7) Quantification of structural features of the toroid:*
>
> *i) Page 5 last sentence mentions that it provides crucial information on the connectivity and length of the filaments. Is it possible to show a quantification of these features in the toroid models?*

Based on our data, we hypothesize that ZapD crosslinks filaments by creating a network of short filaments rather than long ones. These short filaments assemble to form a complete ring. However, the current resolution of the data precludes precise quantification of this process.

In the revised version, we have changed this last sentence to put the emphasis on the crosslinking geometry instead (page 7, lines 40-43):

“Cryo-ET imaging of ZapD-mediated FtsZ toroidal structures revealed a preferential vertical stacking and crosslinking of short ZapD filaments, which are also crosslinked laterally and diagonally, allowing for filament curvature and resulting in a toroidal structure observed for the first time following the interaction between FtsZ and one of its natural partners in vitro.”

> *ii) In toroids with increasing concentrations, will it be possible to quantify the number of blobs which have been interpreted as ZapD? Is this consistent with the data of FtsZ to ZapD ratios?*

These quantifications would assist in interpreting the data. However, due to the limited resolution of the data, we are reluctant to provide estimates.

> *iii) What is the average length of the filaments in the toroid? Can this be quantified from the tomography data? Similarly, can there be an estimation of curvature of the filaments from the data?*

Unfortunately, the complexity of the toroidal structure and the limited resolution we achieved prevent us from providing accurate quantification. We attempted to track and measure the length of the filaments, but this proved challenging due to the high concentration of connections. Regarding curvature, the arrangement of the filaments into toroids makes it difficult to measure the curvature of each filament. Additionally, the filaments are not perfectly aligned, which suggests that there may be various curvatures present.

> *iv) What is the average distance between the FtsZ filaments in the toroid? Does this correlate with the ZapD dimensions, when a model has been interpreted as ZapD?*

We measured the spacing (not the center-to-center distance) between filaments in the toroids and showed this in Supplementary Fig. 14b (sky blue). We observed that the distances are very similar to those found for straight bundles (light blue), with a slightly greater variability. We should point out here that the distances were measured in the XY plane to simplify the measurements.

> *v) What is the estimate of average inter-filament distances within the toroid? (Similar data as in Figure 13 for bundles?) When the distance between filaments is less, is the*

> *angle between ZapD and FtsZ filament axis different from 90 degrees? This might help in validation of interpretation of some of the blobs as ZapD.*

The distances between the filaments presented in Supplementary Figure 14b include those for toroids (1:1 ratio, represented in sky blue) and straight bundles (1:6 ratio, shown in light blue). We focused solely on the distance between filaments in the XY plane and did not differentiate based on the connection angle. Although the distance may vary with changes in the angles between filaments, our data does not permit us to make any quantitative measurements regarding these variations.

> *vi) How does the inter filament distance in the toroids compare with the dimensions of ZapD dimers, in the toroids and bundles? Is there a role played by the FtsZ linker in deciding the spacing?*

The dimension of a ZapD dimer is ~7 nm along the longest axis. Huecas et al. (2017 Biophys J - DOI: 10.1016/j.bpj.2017.08.046) estimated an interfilament distance of ~6.5-6.7 nm for toroids of FtsZ from *Bacillus subtilis*. These authors also observed a difference in this spacing as a function of the linker, assuming that linker length would modulate FtsZ-FtsZ interactions. We observe a similar spacing for double filaments (5.9 ± 0.8 nm) and a longer spacing in the presence of ZapD (7.88 ± 2.1 nm). Previous studies with ZapD did not measure the distance between filaments but hypothesized that distances of 6-12 nm are allowed based on the structure of the protein (Schumacher M. 2017 J Biol Chem - DOI: 10.1074/jbc.M116.773192). Longer linkers may also provide additional freedom to spread the filaments further apart and facilitate a higher degree of variability in the connections by ZapD. This discussion has been included in the revised text (page 6, line 10-18).

> *(8) Crosslinking by ZapD and toroid reorganisation by transient interactions:*
>
> *i) Page 5, paragraph 2: Presence of putative ZapD decorating a single FtsZ': When ZapD is interacting with 2 FtsZ monomers within the same protofilament, it does not have any more valency to crosslink filaments. How do the authors propose that this can connect nearby filaments?*

We thank the reviewer for raising this interesting question. We see examples of ZapD dimers binding a filament through only one of the monomers, occupying one valency of the interaction and leaving one of the monomers available for another binding. We expect to see higher densities of ZapD in the outer regions of toroids simply because there are no longer (or not as frequent) FtsZ filaments available to be attached and join the overall toroid structure. Assuming that a ZapD dimer could bind the same FtsZ filament, this region would not be able to connect to other nearby filaments via these interactions.

> *ii) Page 5: How are the authors coming up with the proposal of a reorganisation of toroid structures to a bundle? Given the extensive cross linking, a transition from a toroid to a bundle has to be a cooperative process and may not be driven by transient interactions. I would imagine that the higher concentration of ZapD will directly result in straight bundles because of the increased binding events of a dimer to one filament.*

Theoretically, this is correct. A certain degree of cooperativity linked to multivalent interactions would also favor the establishment of other ZapD connections. Furthermore, the formation of these structures occurs relatively quickly, within the first two minutes following the addition of GTP. We observed various intermediate structures, ranging from sparse filament bundles to toroids and straight filaments. However, the limited data prevents us from proposing a model that eventually explains the formation of higher-order structures over time.

> *iii) Given such a highly cross-linked mesh, how can you justify transient interactions and loss of ZapD leading to disassembly? The possibility that ZapD can diffuse out of such a network seems impossible. Hence, what is the significance of a transient interaction? What is the basis of calling the interactions transient?*

We have noted that the term “transient” used to define the interaction between ZapD and FtsZ seems to generate confusion. Therefore, we have decided to replace this term to improve the readability of our manuscript, which has been edited accordingly.

> *iv) Does the spacing between ZapD connections decide the curvature of the toroid?*

The FtsZ linker connected to ZapD molecules could modulate filament spacing and curvature, as previously suggested (Huecas et al. 2017 Biophys J - DOI: 10.1016/j.bpj.2017.08.046; Sundararajan and Goley 2017 J Biol Chem - DOI: 10.1074/jbc.M117.809939, and Sundararajan et al. 2018 Mol Microbiol - DOI: 10.1111/mmi.14081). In our structures, we observe a mixture of curvatures in the internal organization of the toroid. Despite the flexibility of FtsZ, filaments have a preferred curvature that FtsZ would initially determine. However, the amount of ZapD connections will eventually force the filament structure to adapt and align with neighboring filaments, facilitating connections with more ZapDs. Thus, the binding density of ZapD molecules significantly impacts FtsZ curvature rather than the ZapD connections themselves. However, the molecular mechanism describing the link between ZapD binding and polymer curvature remains unsolved.

> *v) What is the difference in conditions between supplementary figure 6 and 12? Why is it that toroids are not observed in 12, for the same ratios?*

Both figures show images of samples under the same conditions. At high ZapD concentrations in the sample, we observe a mixture of structures ranging from single filaments, bundles, toroids, and straight bundles. In Supplementary Fig. 6, we have selected images of toroids, while in Supplementary Fig. 12, we have focused on single and double filaments. We aim to compare similar structures at different ZapD concentrations.

> *(9) Correlation with in vivo observations:*
>
> *What is the approximate ratio of ZapD to FtsZ concentrations in the cell? In this context, within a cell which one - a toroid or bundle - will be preferred?*

Previous studies have estimated that *E. coli* cells contain approximately 5,000 to 15,000 FtsZ protein molecules, resulting in a concentration of around 3 to 10 μM (Rueda et al. 2003 J Bacteriol - DOI: 10.1128/JB.185.11.3344-3351.2003). Furthermore, only about two-thirds of these FtsZ molecules participate in forming the division ring (Stricker et al. 2002 PNAS - DOI: 10.1073/pnas.052595099). In contrast, ZapD is a low-abundance protein, with only around 500 molecules per cell (DurandHeredia et al. 2012 J Bacteriol - DOI: 10.1128/JB.00176-12), making it a relatively small fraction compared to the FtsZ molecules. Under these circumstances, toroidal structures are more likely to form than straight bundles, as the latter would require significantly higher concentrations of ZapD for proper assembly. We have added these considerations in the revised text (page 11, lines 1-7).

> *(10) Interpretation of mZapD results:*
>
> *i) What is the experimental proof for weakened stability of the dimer? Rather than weakened stability, does this form a population of only monomeric ZapD or a proportion of non-functional or unfolded dimer? This requires to be shown by AUC or SEC to substantiate the claim of a weakened interface.*

We have provided new AUC results indicating that mZapD is partially monomeric, which suggests a weakened dimerization interface (page 9, line 15-16 and Supp. Fig. 15a). The assays revealed no signs of protein aggregation.

> *ii) How does a weaker dimer result in thinner bundles and not toroids? A weaker dimer would imply that the number of ZapD linked to FtsZ will be less than the wild type, leading to less cross linking, which should lead to toroid formation rather than thinner bundles.*

This observation provides the most plausible explanation. However, we did not detect any toroidal structures, even at high concentrations of mZapD. This finding indicates that a more potent dimerization interface is essential for promoting the formation of toroidal structures rather than merely the number of ZapD-FtsZ connections. mZapD presumably has a reduced affinity for FtsZ, which, along with a weaker binding interface, may explain mZapD's inability to facilitate toroid formation.

> *iii) This observation would imply that the geometry of the dimeric interaction plays a role in the bending of the FtsZ filaments into toroids? Please comment.*

Our data suggest that the binding density of ZapD to FtsZ polymers is a crucial factor governing the transition from toroidal structures to straight bundles. Toroids form when the polymers have excess free FtsZ (that ZapD does not crosslink). Additional factors, such as the orientation of the interactions, the length of the flexible linker, and the strength of the ZapD dimerization interface, are likely to contribute to these structural reorganizations. However, our current data do not allow for further analysis, and future experiments will be necessary to address these questions.

> *(11) Curvature and plasticity of toroid:*
>
> *i) What are the factors that stabilise curved protofilaments/toroid structures in the absence of a cross linker, based on earlier studies from B. subtilis. A comparison will be insightful. ii) What is the effect of the linker length between FtsZ globular domain and CTP in the toroid spacing?*

Huecas et al. 2017 (Biophys J - DOI: 10.1016/j.bpj.2017.08.046) concluded that the disordered CTL of FtsZ serves as a spacer that modulates the self-organization of FtsZ polymers. They proposed that this intrinsically disordered CTL, which spans the gap between protofilament cores, provides approximately 70 Å of lateral spacing between the curved *Bacillus subtilis* FtsZ (BsFtsZ), forming toroidal structures. In contrast, the parallel filaments of tailless BsFtsZ mutants, which have a reduced spacing of 50 Å, will likely stick together, resulting in the straight bundles observed. In the full-length BsFtsZ filament, the flexibility allowed by the lateral association favors the coalescence of these curved protofilaments, leading to the formation of toroidal structures.

The role of the C-terminal tail of FtsZ in *E. coli* is critical for its functionality (Buske and Levin 2012 J Biol Chem - DOI: 10.1074/jbc.M111.330324). However, its structural involvement in complex formations remains unclear. Research indicates that any disordered peptide between 43 and 95 amino acids in length can function as a viable linker, while peptides that are significantly shorter or longer impede cell division (Gardner et al. 2013 Mol Microbiol - DOI: 10.1111/mmi.12279). Studies in *E. coli* and *B. subtilis* suggest that intrinsically disordered CTLs play a role in determining FtsZ assembly and function *in vivo*, and this role is dependent on the length, flexibility, and disorder of the tails. These aspects still require further exploration.

> *iii) How is it concluded that the concentration of ZapD is modulating the behaviour of the toroid structure? ZapD as a molecule does not have much room for conformational flexibility beyond a few angstroms, in the absence of long flexible regions. Rather, shouldn't the linker length of FtsZ to the CTP decide the plasticity of the toroid?*

The length and flexibility of the linker can significantly influence structural interactions. As previously mentioned, a longer linker will likely enhance the range of interaction distances and orientations. However, specific interaction of ZapD and FtsZ is stronger than non-specific electrostatic FtsZ-FtsZ interactions, and this is not solely due to the flexibility of the linker. Instead, it can modulate the formation of either a toroidal structure or straight bundles.

> *iv) "a minor free energy perturbation to bring about significant changes in the geometry of the fibers due to modifications in environmental conditions" - this sentence is not clear to me. How did the data described in the paper relate to minor free energy perturbations and how do environmental conditions affect this?*

This sentence aimed to convey the notion of polymorphism in FtsZ polymers. We acknowledge that the original version may have been unclear, so we have removed it in the new version of the manuscript (page 12, lines 1-2).

> *(12) Missing controls:*
>
> *i) Supplementary Figure 2a: Interaction between ZapD and FtsZ: what was the negative control used in this experiment? Use of FtsZ with the CTP deletion or ZapD specific mutations will help in confirming that the Kd estimation is indeed driven by a specific interaction.*

Negative controls correspond to FtsZ and ZapD alone.

> *ii) In a turbidity measurement, how will you distinguish between ZapD mediated bundling, ZapD independent bundling and FtsZ filaments alone? Here again, having a data with non-interacting mutational partners will make the data more reliable.*

The turbidity signal of individual proteins in the absence and presence of GTP is indistinguishable from that of the buffer. We have indicated this in the figure legend.

> *iii) Control experiments to show that mZapD is folded (see point below) and to indeed prove that it is monomeric is missing.*

We have included the missing AUC data in the supplementary information (Supp Fig 15a).

> *Minor points:*
>
> *- Page 2, para 4: beta-sheet domain (instead of beta-strand)*

Done.

> *- Fig 2a and b: Why is a ratio mentioned in Figure 2a legend? I understood these images as individual proteins at 10 uM concentrations.*

That was a typing error; it corresponds to two individual proteins at 10 μM concentrations.

> *- Fig 2. Y-axis - spelling of frequency (change in all figures where applicable)*

Corrected.

> *- Supplementary Figure 5: FtsZ 5 uM - change u to micro symbol. FtsZ - t is missing*

Corrected.

> *- Molecular weight marker is xx. What does xx stand for?*

Corrected.

> *- Fig 1: Units for GTPase activity on the y-axis is missing.*

Done.

> *- Suppl Fig 3: How was the normalisation carried out for the turbidity data?*

We have explained it the revised methods section.

> *- Page 4, line 5: p missing in ZapD*

Done.

> *- Page 5: paragraph 1, last sentence: stabilised or established?*

Done.

> *- Page 6: 3rd sentence from last: correct the sentence (one ZapD two FtsZ)*

Corrected.

> *- Page 14: Fluorescence microscopy and FRAP experiments have not been described in the manuscript. Hence, these are not required in the methods.*

Corrected.

> *- Please include representative gels of purified protein samples used in the assay for sample quality control.*

Controls for each protein are shown in Supplementary Fig. 5a as “control samples” corresponding to 5 μM of each protein before centrifugation.

> ***Reviewer #3 (Recommendations for the authors):***
>
> *Fig. S2a confirms and quantitates the interaction of ZapD with FtsZ-GDP monomers by F.A. It shows a surprisingly high Kd of ~10 μM. This seems important but it is ignored in the overall interpretation. Fig. S2b (FCS) suggests an even weaker interaction, but this may reflect higher order aggregates.*

As the reviewer points out, the interaction between ZapD and FtsZ in the GDP form is weak, consistent with the need for high concentrations of ZapD to form FtsZ macrostructures in the presence of GTP.

We did not observe the formation of ZapD aggregates, even at higher protein (Author response image 1A) and salt (Author response image 1B) concentrations.

Author response image 1.

A) Sedimentation velocity (SV) profiles of ZapD over a concentration range of 2 to 30 μM in 50 mM KCl, 5 mM MgCl2, Tris-HCl pH 7. B) SV profiles of ZapD at 10 μM in different ionic strength concentrations in buffer 50-500 mM KCl, 5 mM MgCl2, 50 mM Tris-HCl pH 7. Abs280 measurements were collected at 48,000 rpm and 20 ºC.

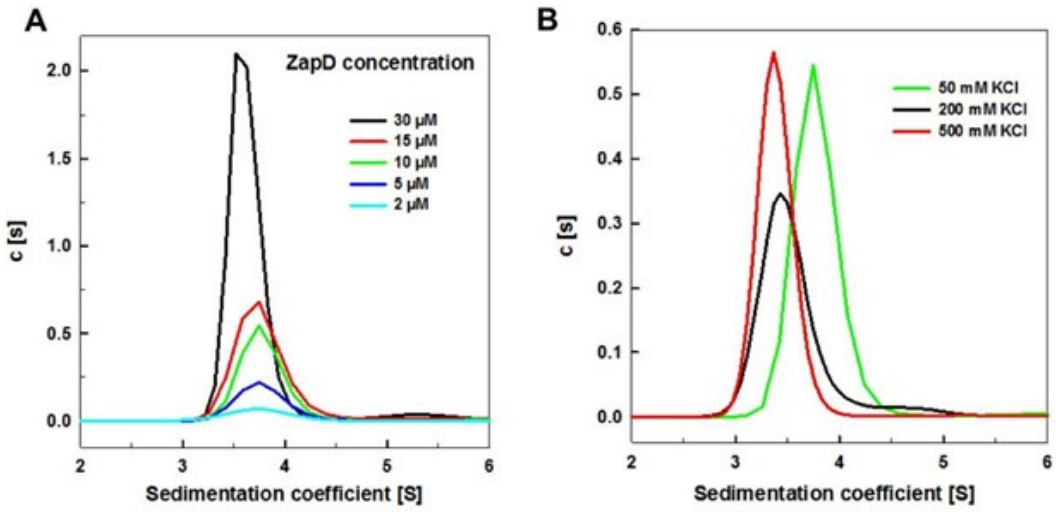

> *Describing their assembly of toroids the authors state "Upon adding equimolar amounts of ZapD, corresponding to the subsaturating ZapD binding densities described in the previous section". My reading of Fig. 1b and S5 is that FtsZ is almost fully saturated at 1:1 concentration; In S5a at 5:5 μM about 25% of each is in the pellet, which is near 1:1 saturation. It is certainly >50% saturated. Shouldn't this be clarified to read "slightly substoichiometric. Of course, that undermines the identification of ZapD as such a substoichiometric number.*

We have rephrased the sentence following the reviewer's suggestions to clarify matters (page 5, lines 39-40).

> *The cryoET images in Fig. 3 are an average of five slices with a total thickness of 32 nm. The circular "short filaments..almost parallel" are therefore not single 5 nm diameter FtsZ filaments but must be alignment of filaments axially into sheets (or belts, the axial structure shown in Fig. S8e, discussed next). Importantly, the authors indicate "connections between filaments" by red arrows. This seems wrong for two reasons. (1) The "connections" are very sparse, and therefore not consistent with the near saturation of FtsZ by ZapD. (2) To show up in the 32 nm averaged slice, connections from multiple filaments would have to be aligned. Fig. 3e is a "view of the segmented toroidal structure." I think it shows sheets of filaments as noted above, and the suggested "crosslinks" are again very sparse and no more convincing.*

We thank the reviewer for pointing this out. This was an error on our part, which we have corrected in the figure legend of the revised version of the manuscript. The tomographic slice shown in Fig. 3a is an average of 5 slices, each with a pixel size of 0.86 nm, corresponding to a pixel size of 4.31 nm. It therefore corresponds to the thickness of a single FtsZ filament. The few red arrows indicate lateral connections between filaments, and as discussed earlier, ZapDs also crosslinks FtsZ filaments vertically, giving rise to the elongated structures observed in the Z-direction.

> *All 3-D reconstructions and segmented renditions should have a scale bar. The axial cylindrical sheets seem to be confirmed and qualified in Fig. S8e. The cylindrical sheets are not continuous, but seem to consist of belt-like filaments that are ~8-10 nm wide in the axial direction. Adjacent belts are separated axially by ~5 nm gaps, and radially by 4-20 nm. The densest filaments in the projection image Fig. 3b are probably an axial superposition of 2-3 belts, while the lighter filaments may be individual belts.*
>
> *Fig. 4 shows a higher number of crosslinks but nowhere near a 1:1 stoichiometry. Most importantly to me, the identification of crosslinks vs filaments seems completely arbitrary. For example, if one colored grey all of the densities I 4a right panel, I would have no way to duplicate the distinctions shown in red and blue. Even if we accept the authors' distinction, it does not provide much structural insight. Continuous bands or sheets are identified as FtsZ, without any resolution of substructure, and any density outside these bands is ZapD. The spots identified as ZapD seem randomly dispersed and much too sparse to include all the ~1:1 ZapD.*

We appreciate the reviewer's comments. Scale bars are present in the tomographic slices but not in the 3D views, as these are perspective views, and it would be inappropriate to include scale bars. To provide context for the images, we added the dimensions of the toroids and toroid sections to the figure legends.

As previously mentioned, the resolution of our data limits our ability to accurately segment ZapD densities, especially in the Z direction. In Fig. 4, we have done our best to segment the ZapD densities at the top and sides of the FtsZ filaments, but many densities have been missed. We have clarified this point in the text and in the figure legend. We have clarified this point in both the text and the figure legends. This preliminary annotated view is meant to help illustrate the formation of the toroids. In Fig. 3, we have labeled only a few arrows to highlight the lateral connections between the FtsZ filaments; however, there are many more connections than those indicated.

> *Fig. S12 explores the effect of increasing ZapD to 1:6, and the authors conclude "the high concentration of ZapD molecules increased the number of links between filaments and ultimately promoted the formation of straight bundles." However, the binding sites on FtsZ are already nearly saturated at 10:10.*

We cannot assume that all FtsZ binding sites are present at a 1:1 ratio. Our pelleting assay confirms the presence of both proteins in the pellet, but we should be cautious about quantification due to the limitations of this technique. Based on our cryo-EM experiments, the amount of ZapD associated with these structures is much lower. We hypothesize that ZapD proteins sediment with the large FtsZ structures, acting as an external decoration for the toroids. A single ZapD monomer may be bound to multiple outer filaments of the structures, which could effectively increase the total μM concentration observed in the pelleting assay. This situation may explain the enrichment of ZapD in the pellet at high concentrations, when theoretically only a 1:1 ratio should be possible. We have observed external decorations of ZapD at high concentrations (see Supplementary Fig. 6). We believe that the pelleting assay simplifies the system and should be used to complement the cryo-EM images.

> *Minor points.*
>
> *In the Intro "..to follow a treadmilling behavior, similar to that of actin filaments.9-13." These refs have little to do with treadmilling. I suggest: Wagstaff..Lowe mBio 2017; Du..Lutkenhaus PNAS 2018; Corbin Erickson BJ 2020; Ruis..Fernandez-Tornero Plos Biol 2022.*

Following the reviewer's suggestions, we have modified the references in the revised version.

> *The authors responded to a query during review stating that the concentration of ZapD always refers to the monomer subunit. That seems certainly the case for Fig. S1, but the caption to Fig. 1a confuses the stoichiometry issue: "expecting (sic) at around 2:1 FtsZ:ZapD." Perhaps it could be clarified by stating that the Fig. shows only half the FtsZ's occupied. But in Fig. 1b the absorbance reaches its maximum at equimolar FtsZ and ZapD. That means that all FtsZ's are bound to a ZapD monomer. Why not draw the model in 1A show that? Fig. S5 is also consistent with this 1:1 stoichiometry. And this might be the place to contrast the planar model with the stacked model suggested by Fig. 5 where the two FtsZ filaments are ~8 nm apart, and the ZapD bridging them is on top.*

We have revised the legend for Fig. 1a to improve its readability. In Fig. 1b, the absorbance data indicate that most FtsZ proteins form macrostructures; however, this does not imply that all FtsZ proteins are bound to ZapDs. Our findings demonstrate that this binding only occurs in the case of straight bundles.

> *It may help to note that some previous studies have expressed the concentration of ZapD as the dimer. E.g., Roach..Khursigara 2016 found maximal pelleting at FtsZ:ZapD(dimer) of 2:1 (their Fig. 3), completely consistent with the 1:1 FtsZ:ZapD(monomer) in the present study.*

We recognize this discrepancy in the literature. Therefore, throughout the manuscript, the molar concentrations of both proteins are expressed in terms of the FtsZ and ZapD monomer species.

https://doi.org/10.7554/eLife.95557.2.sa0